frontiers in Aging Neuroscience

ORIGINAL RESEARCH
published: 25 May 2020
doi: 10.3389/fnagi.2020.00140

Vitamin D, Folate, and Cobalamin Serum Concentrations Are Related to Brain Volume and White Matter Integrity in Urban Adults

May A. Beydoun[1†], Danielle Shaked[1,2], Sharmin Hossain[1], Hind A. Beydoun[3], Leslie I. Katzel[4,5], Christos Davatzikos[6], Rao P. Gullapalli[7], Stephen L. Seliger[8], Guray Erus[6], Michele K. Evans[1], Alan B. Zonderman[1] and Shari R. Waldstein[2,4,5]*

[1] Laboratory of Epidemiology and Population Sciences, The National Institute on Aging (NIA) The Intramural Research Program (IRP), The National Institutes of Health (NIH), Baltimore, MD, United States, [2] Department of Psychology, University of Maryland, Baltimore County, MD, United States, [3] Department of Research Programs, Fort Belvoir Community Hospital, Fort Belvoir, VA, United States, [4] Geriatric Research Education and Clinical Center, Baltimore VA Medical Center, Baltimore, MD, United States, [5] Division of Gerontology & Geriatric Medicine, Department of Medicine, University of Maryland School of Medicine, Baltimore, MD, United States, [6] Section for Biomedical Image Analysis, Department of Radiology, University of Pennsylvania, Philadelphia, PA, United States, [7] Department of Diagnostic Radiology, University of Maryland School of Medicine, Baltimore, MD, United States, [8] Division of Nephrology, Department of Medicine, University of Maryland School of Medicine, Baltimore, MD, United States

OPEN ACCESS

Edited by:
Dennis Qing Wang, Southern Medical University, China

Reviewed by:
Goran Simic, University of Zagreb, Croatia
Tzvi Dwolatzky, Technion Israel Institute of Technology, Israel

***Correspondence:**
May A. Beydoun
baydounm@mail.nih.gov

†MB had full access to the data used in this manuscript and completed all the statistical analyses

Received: *20 February 2020*
Accepted: *27 April 2020*
Published: *25 May 2020*

Citation:
Beydoun MA, Shaked D, Hossain S, Beydoun HA, Katzel LI, Davatzikos C, Gullapalli RP, Seliger SL, Erus G, Evans MK, Zonderman AB and Waldstein SR (2020) Vitamin D, Folate, and Cobalamin Serum Concentrations Are Related to Brain Volume and White Matter Integrity in Urban Adults. Front. Aging Neurosci. 12:140. doi: 10.3389/fnagi.2020.00140

Background and objectives: Lower vitamin status has been linked to cognitive deficits, pending mechanistic elucidation. Serum 25-hydroxyvitamin D [25(OH)D], folate and cobalamin were explored against brain volumes and white matter integrity (WMI).

Methods: Two prospective waves from Healthy Aging in Neighborhoods of Diversity Across the Life Span (HANDLS) study were primarily used [Baltimore, City, MD, 2004–2015, N = 183–240 urban adults (Age_{v1}: 30–64 years)]. Serum vitamin 25-hydroxyvitamin D [25(OH)D], folate and cobalamin concentrations were measured at visits 1 (v_1: 2004–2009), while structural and diffusion Magnetic Resonance Imaging (sMRI/dMRI) outcomes were measured at vscan: 2011–2015. Top 10 ranked adjusted associations were corrected for multiple testing using familywise Bonferroni (FWER $<$ 0.05) and false discovery rates (FDR, q-value $<$ 0.10).

Results: We found statistically significant (FWER $<$ 0.05; β±SE) direct associations of 25(OH)D(v_1) with WM volumes [overall: +910 ± 336/males: +2,054 ± 599], occipital WM; [overall: +140 ± 40, males: +261 ± 67 and Age_{v1} $>$ 50 years: +205 ± 54]; parietal WM; [overall: +251 ± 77, males: +486 ± 129 and Age_{v1} $>$ 50 years: +393 ± 108] and left occipital pole volume [overall: +15.70 ± 3.83 and above poverty: 19.0 ± 4.3]. Only trends were detected for cobalamin exposures (q $<$ 0.10), while serum folate (v_1) was associated with lower mean diffusivity (MD) in the Anterior Limb of the Internal Capsule (ALIC), reflecting greater WMI, overall, while regional FA (e.g., cingulum gyrus) was associated with greater 25(OH)D concentration.

Conclusions: Among urban adults, serum 25(OH)D status was consistently linked to larger occipital and parietal WM volumes and greater region-specific WMI. Pending longitudinal replication of our findings, randomized controlled trials of vitamin D supplementation should be conducted against brain marker outcomes.

Keywords: 25-hydroxyvitamin D, folate, cobalamin, brain volumes, white matter integrity, cognitive aging, health disparities

INTRODUCTION

A possible beneficial effect of several vitamins on cognition has been suggested (Beydoun et al., 2014a). Vitamin D is a steroid hormone that regulates calcium homeostasis. Serum 25-hyrdoxyvitamin D [25(OH)D], or vitamin D status, is primarily determined by sunlight skin exposure and secondarily by dietary and supplemental intakes (Buell and Dawson-Hughes, 2008). Vitamin D's active form (1,25-dihydroxyvitamin D_3) maintains and stabilizes intracellular signaling pathways involved in memory and cognition (Eyles et al., 2013) by increasing *VDR* (Guo et al., 2016) and *LRP2* expression in the choroid plexus and helping clear neurotoxic β-amyloids (Deane et al., 2004; Carro et al., 2005) involved in Alzheimer's disease (AD) pathogenesis (Roher et al., 1993). Vitamin D-related gene polymorphisms and lower vitamin D intake and status were linked to cognitive decline in epidemiological studies (Annweiler et al., 2016; Kuzma et al., 2016; Beydoun et al., 2018; Goodwill et al., 2018) and to markers of brain atrophy and poor white matter integrity (WMI) (Buell et al., 2010; Annweiler et al., 2013, 2015b; Michos et al., 2014; Prager et al., 2014; Brouwer-Brolsma et al., 2015; Del Brutto et al., 2015; Moon et al., 2015; Karakis et al., 2016; Littlejohns et al., 2016; Al-Amin et al., 2019). Vitamin D's neuroprotective role is likely mediated through the expression of neurotrophins, neurotransmitters, and suppression of inflammatory cytokines (Buell and Dawson-Hughes, 2008; Miller, 2010; Etgen et al., 2012).

Moreover, folate and cobalamin (vitamin B-12) are essential in remethylation of homocysteine (Hcy), a sulfur amino acid with neurotoxic and excitotoxic properties (Kruman et al., 2000), yielding methionine (Bottiglieri, 2005; Troesch et al., 2016). Hcy was recently shown in animal studies to increase tau protein phosphorylation, truncation, and oligomerization, an evidence of direct involvement in AD's second pathological hallmark, namely neurofibrillary tangles (NFTs) (Shirafuji et al., 2018). Hcy is also converted to cysteine via a vitamin B6-dependent mechanism (Troesch et al., 2016). Importantly, folate and cobalamin status were inversely associated with age-related cognitive decline (McCaddon and Miller, 2015; Smith and Refsum, 2016), with cobalamin further exhibiting direct associations with brain volumes and WMI (Erickson et al., 2008; Vogiatzoglou et al., 2008; De Lau et al., 2009; Pieters et al., 2009; Lee et al., 2016). A recent trial demonstrated beneficial effects of B-vitamin supplementation on brain magnetic resonance imaging (MRI) measures and cognitive function longitudinally (De Jager et al., 2012; Douaud et al., 2013). Furthermore, nutritional biomarkers may work synergistically to improve cognitive outcomes (Min and Min, 2016; Moretti et al., 2017). Since socio-demographic factors relate to both nutrition and cognition (Beydoun et al., 2014b; Berg et al., 2015; McCarrey et al., 2016; Weuve et al., 2018), studying relations of vitamin D, folate and cobalamin with brain MRI measures, while stratifying by relevant sociodemographic factors is key.

This study examines associations of serum 25(OH)D, folate and cobalamin concentrations with brain volume and WMI among a diverse sample of urban adults, while stratifying by sex, age, race, and poverty status. We hypothesized that first-visit serum 25(OH)D, folate, and cobalamin (and annual rate of change over time) would directly correlate with global and regional gray and white matter (WM and GM) brain volumes and regional WMI measured at one follow-up visit (v_{scan}), after a mean follow-up of 5.7 years. Analyses also explored brain regions' sensitivity to lower vitamin status, differentially by socio-demographic factors.

METHODS AND MATERIALS

Database

Using area probability sampling, a socio-demographically diverse sample of middle-aged White and African-American urban adults (Age v_1: 30–64 years) from thirteen contiguous census tracts of Baltimore was recruited into the Healthy Aging of Neighborhoods of Diversity across the Life Span (HANDLS) study (Evans et al., 2010). HANDLS is an on-going prospective cohort study, initiated in 2004 by the National Institute on Aging. Potential participants were interviewed and identified by random selections of address listings within each census tract (Evans et al., 2010). Participants were invited to join HANDLS if they met the following criteria: (1) between ages 30–64; (2) not currently pregnant; (3) not within 6 months of active cancer treatment; (4) not diagnosed with AIDS; (5) capable of providing written

Abbreviations: AA, African Americans; ALIC, Anterior Limb of the Internal Capsule; C-TRIM, Core for Translational Research in Imaging @ Maryland; DTI, Diffusion Tensor Imaging, dMRI, Diffusion MRI; FA, Fractional Anisotropy; FWER, Familywise Error Rate, FDR, False Discovery Rate; FLAIR, Fluid-Attenuated Inversion Recovery; FOV, Field of View; GM, Gray Matter; HANDLS, Healthy Aging in Neighborhoods of Diversity across the Life Span study; HS, High School; LRP2, Megalin gene; MP-RAGE, Magnetization prepared rapid gradient echo; MRI, Magnetic Resonance Imaging; MD, Mean Diffusivity; MRV, Medical Research Vehicle; MMSE, Mini-Mental State Examination; MICO, Multiplicative intrinsic component optimization; MUSE, Multi-atlas region Segmentation utilizing Ensembles; OCM, One-Carbon Metabolism; ROI, Regions of Interest; 25(OH)D, Serum 25-hydroxyvitamin D; FOL, Serum folate; B-12, Serum vitamin B-12; Hcy, Homocysteine; SA, Sensitivity Analysis; sMRI, Structural MRI; TR, TRACE; US, United States; *VDR*, Vitamin D receptor gene; WMI, White Matter Integrity; WM, White Matter.

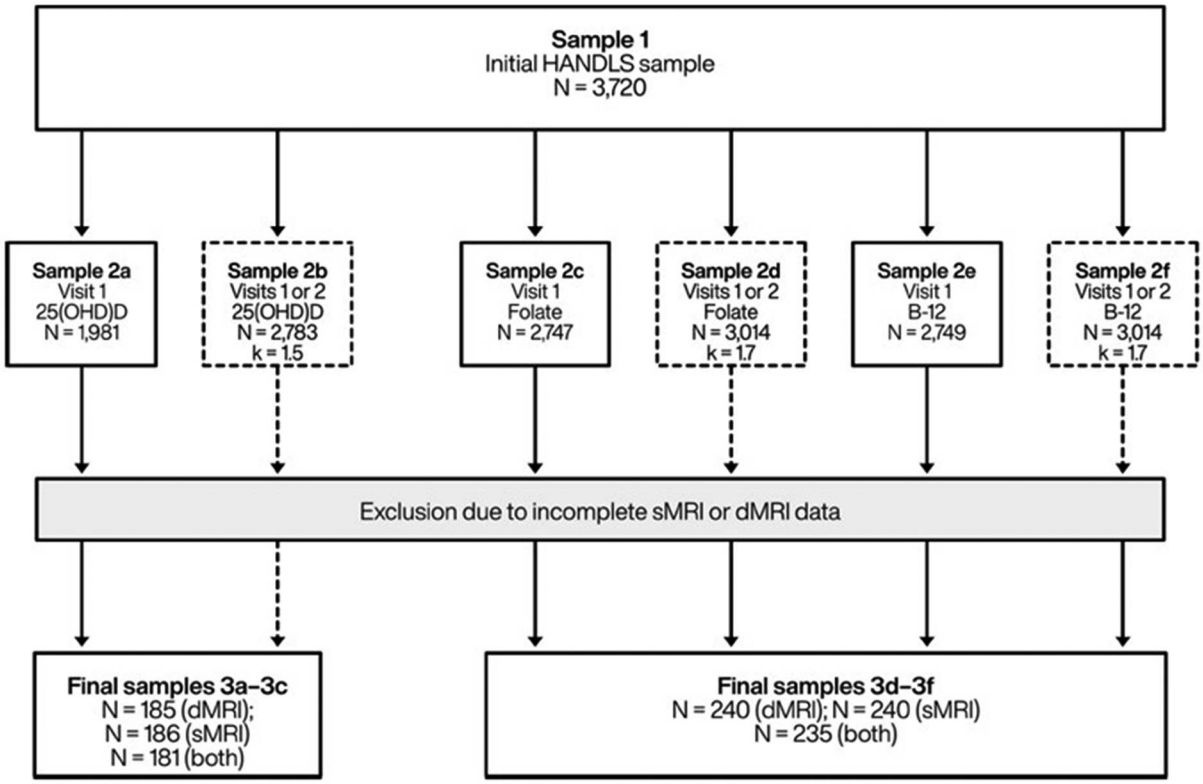

FIGURE 1 | Study participant schematic: HANDLS 2004–2013 and HANDLS-SCAN 2011–2015[a]. 25(OH)D, 25-hydroxyvitamin D; B-12, Vitamin B-12 (cobalamin); dMRI, Diffusion magnetic resonance imaging; HANDLS, Healthy Aging in Neighborhoods of Diversity Across the Life Span; κ, average number of repeats; sMRI, Structural/volumetric magnetic resonance imaging. [a]Visit 1 refers to HANDLS 2004–2009; Visit 2 refers to HANDLS 2009–2013; and HANDLS-SCAN visit (v_{scan}) was carried out between 2011 and 2015.

informed consent, thus excluding individuals with probable dementia or very low literacy among others; (6) with a valid government-issued identification and a verifiable address (Evans et al., 2010).

Initial examinations were performed in two phases. Phase 1 included the first dietary interview and completion of various demographic and psychosocial scales. Phase 2, performed on Medical Research Vehicles (MRV) parked in participants' neighborhoods, included the second dietary interview and various physical, medical, and psychosocial examinations, including DXA for bone mineral density and body composition, EKG, intima-media thickness by ultrasound, personal and family health history, physical examination by a physician, physical performance by a brief screening battery, neuropsychological tests, and inventories to assess depressive symptoms (Evans et al., 2010). Follow-up visits included largely comparable MRV visits. At visit 2 (v_2, 2009–2013), blood draw analyzed in the same laboratory facility as for visit 1 yielded similar biochemical and hematological indices that can be studied longitudinally.

Written informed consent was obtained from all participants. Study protocols for HANDLS and HANDLS SCAN were approved by the National Institute on Environmental Health Sciences Institutional Review Board (IRB) of the National Institutes of Health. HANDLS SCAN was also approved by the IRBs of the University of Maryland School of Medicine and the University of Maryland, Baltimore County.

This study analyzed nutritional biomarker data from visit 1 (v_1: 2004–2009) in relation to follow-up data measured in a subsample of $N_{max} = 258$ participants within the HANDLS SCAN sub-study (vscan: 2011–2015) (Waldstein et al., 2017). Exposure variables were measured during the Medical Research Vehicle (MRV) examinations; outcomes were MRI measures of brain volume and WMI at vscan (Waldstein et al., 2017). The mean follow-up time between visit 1 and vscan was 5.70 years ± 1.90.

Study Sample

The initial HANDLS cohort included 3,720 participants (30–65 years, AAs and Whites, Phase I, visit 1). We included participants with complete and valid MRI data at follow-up and complete 25(OH)D, folate and cobalamin data at visit 1 and/or visit 2 (**Figure 1**). Mean ± SD of follow-up time between v_1 and v_2 was 4.65 years ± 0.93 (range: 0.4–8.2 years). The final sample was reduced to $N = 185$–186 for vitamin D and $N = 240$ for folate or cobalamin exposures.

Brain sMRI

A Siemens Tim-Trio 3.0 Tesla scanner was used for MRI assessments. Magnetization prepared rapid gradient echo (MP-RAGE) was used to perform volumetric measurements for anatomical regions. Volumetric measures were estimated for each region of interest (ROI). Detailed description is provided in **Supplemental Method 1**.

In addition to standard axial T1, T2, FLAIR images, a high-resolution axial T1-weighted MPRAGE (TE = 2.32 ms, TR = 1900 ms, TI = 900 ms, flip angle = 9°, resolution = 256 × 256 × 96, FOV = 230 mm, sl. Thick. = 0.9 mm) of the brain was acquired for structural imaging. Images were used as anatomic references and to extract parameters of regional and whole brain volumes (see **Supplemental Table 1**). This study comprehensively examines brain volumes at ascending segmentation levels.

Brain dMRI

dMRI was obtained using multi-band spin echo EPI sequence with a multi-band acceleration factor of three (**Supplemental Method 1**). Fractional Anisotropy (FA) and trace (TR, aka mean diffusivity or MD) images were computed from tensor images. As intact WM generally allows for more restricted diffusion, higher FA values are indicative of healthier WMI. Summing eigenvalues for diffusion tensor yields MD, with higher values indicative of poorer WMI (Jones, 2008). Computed FA and MD images were aligned to a common template space via deformable registration using a standard dMRI template (i.e., EVE Wakana et al., 2004). Right and left FA and MD values were averaged for each ROI (see **Supplemental Table 2** for list of ROIs).

Vitamin Status Measures

Participants were asked to fast for ≥8 h prior to the MRV visits, and specimens in volumes of 2 mL serum were collected and frozen at −80°C. Similar procedures were adopted for v_1 and v_2 serum folate and cobalamin, measured using chemiluminescence immunoassay[1] by Quest Diagnostics, Chantilly, VA[2], and previously validated against other automated methods with coefficient of variation (CV) < 10% (Owen and Roberts, 2003; Ispir et al., 2015).

25(OH)D were measured using slightly different methodologies between v_1 and v_2. For both visits, blood samples drawn at examination were stored at −80°C. At v_1, total levels of serum 25(OH)D (in ng/ml; D_2 and D_3) were measured using tandem mass spectrometry (interassay CV, 8.6%) at Massachusetts General Hospital, <60 days later, as recommended for frozen samples (Powe et al., 2013). V_2 25(OH)D was measured by Quest Diagnostics (Chantilly, VA) using an immunoassay that includes competitive binding of serum 25(OH)D and tracer-labeled 25(OH)D to specific antibody followed by detection and quantitation via chemiluminescence reaction (Diasorin, formerly Incstar), comparable to National Health and Nutrition Examination Surveys 2003–04 assays[3] (interassay CV: 4–13%) (Centers for Disease Control Prevention, 2006; Diagnostics, 2019)[4].

Dietary and supplemental intakes of vitamin D, folate and cobalamin were shown to moderately correlate with their corresponding serum biomarkers in HANDLS and national surveys (Beydoun et al., 2010a,b, 2018). Moreover, moderate-to-strong correlations were detected for all three biomarkers (Pearson's $r > 0.30$), notably v_1 vs. v_2 values for each vitamin in the HANDLS sample: 25(OH)D ($r = 0.44$, $n = 1{,}462$); folate ($r = 0.44$, $n = 1{,}944$); cobalamin ($r = 0.55$, $n = 1{,}994$). We also describe categorical exposures with cutoffs reflecting vitamin insufficiency or deficiency (Snow, 1999; Thacher and Clarke, 2011; World Health Organization, 2015).

Covariates

All models were adjusted for baseline examination age (y), sex (male = 1, female = 0), race (AA = 1, White = 0), self-reported household income either <125% or ≥125% of the 2004 Health and Human Services poverty guidelines (termed poverty status) (US Department of Health & Human Services, 2019), and time (days) between baseline MRV visit and MRI scan visit. Models were independently stratified by age (≤ 50 vs. >50 years), sex, race, or poverty status. Additional covariates were entered in a sensitivity analysis when independently associated with each exposure of interest (see **Supplemental Method 2**).

Statistical Analysis

Analyses were conducted using Stata version 16.0 (Stata, 2019). First, selected sample characteristics were described, and their means and proportions across key socio-demographic groups were calculated. *T*-test, chi-square, multiple linear, and logistic regression models (Wald tests) were used to determine group differences in distributions of continuous and categorical variables. Second, several sets of analyses were conducted to test main hypotheses, both overall and stratified by age group (≤50 vs. >50 years), sex, race, or poverty status. Ordinary least square regression models included each v_1 vitamin exposure predicting each MRI measure as the outcome measured at v_{scan}, while adjusting for socio-demographic confounders. Ultimately, the most significant adjusted associations with the lowest *p*-values [or highest $-\text{Log}_{10}(p)$] per analysis were selected, along with their unstandardized (β±SE) and standardized (*b*) effect sizes. Consequently, a looping procedure (*parmsby* command) was applied to generate main parameter estimates, interpreted as change in MRI measure per unit change in serum vitamin biomarker for β and fraction of a SD change in MRI measure per 1 SD change in that biomarker for *b*, which was moderate-to-strong if >0.20, and weak-to-moderate if between 0.10 and 0.20. Four separate analyses were conducted based on MRI variable

[1]Siemens Centaur. Available online at: https://www.siemens-healthineers.com/en-us/immunoassay/systems.

[2]Diagnostics, Q. *Vitamin B-12 (Cobalamin) and Folate Panel*. Available online at: https://testdirectory.questdiagnostics.com/test/test-detail/7065/vitamin-b12-cobalamin-and-folate-panel-serum?cc=MASTER (accessed October 21, 2019).

[3]NHANES 2003–2004. Available online at: https://www.cdc.gov/nchs/data/nhanes/nhanes_03_04/l06vid_c_met_Vitamin_D.pdf (accessed December 16, 2019).

[4]Diasorin. Available online at: https://diasoringroup.com/en?gclid=EAIaIQobChMI3JLjuq265gIVhIvICh3G-QcTEAAYASAAEgLz-fD_BwE (accessed December 16, 2019).

groupings. The first analysis included total brain volume (i.e., WM + GM), WM and GM volumes as the only 3 exposure measures (**Model A**). The second analysis included 8 measures (**Model B**): the combination of WM and GM of the 4 main cortical regions: frontal, temporal, parietal, and occipital lobes. A third analysis included the smaller regions, accounting for bilateral volumes, yielding 142 outcome measures (**Model C**). Finally, dMRI measures were included, after taking the average between the left and right side for FA and MD measures, as done previously (McKay et al., 2019). This exploratory approach was conducted previously by at least one other study of vitamin D deficiency and WMI (Moon et al., 2015). This resulted in 98 (49 FA and 49 MD) dMRI outcome measures, reflecting WMI (**Model D**).

For uncorrected *p*-values, Type I error <0.05 was used for significance. To adjust for multiple testing two methods were used: (1) Familywise Bonferroni (error rate) correction (FWER) which adjusted for multiplicity in brain MRI measures, assuming each set of modeling approach (Models A-D and stratification status) applied to each serum vitamin [25(OH)D, folate and cobalamin] to be separate hypotheses, (2) false discovery rate (*q*-value) which only considered the four approaches/stratification status as separate hypotheses (i.e., Models A-D, and stratification status), thus combining the 3 vitamin exposures upon correction. Moreover, the top 10 adjusted associations from each analysis were presented if $p_{\text{uncorr}} < 0.05$, showing the main parameter estimate and its standard error (SE), the uncorrected *p*-values, the FDR *q*-values and FWER status (Yes = passed correction, No = did not pass) and the standardized effect size *b*. Top 10 associations were considered statistically significant if passing FWER correction for a specific vitamin, model and stratification status (yes vs. no) at type I error of 0.05. Results with FDR *q*-value < 0.10 per model and stratification status while failing the FWER criterion were considered a trend. Additionally, when passing FDR *q*-value correction at type I error of 0.10 per vitamin, model and stratification status while failing the FWER criterion, an effect was considered a trend if $|b| \geq 0.20$. Among selected stratified models (top 10 findings), formal effect modification testing was conducted by including 2-way interaction terms between exposure and each socio-demographic factor in the non-stratified model. A Type I error of 0.10 was used for 2-way interaction terms due to reduced statistical power (Selvin, 2004). In addition, the main analyses with v_1 exposures and minimal socio-demographic adjustment, sensitivity analyses were conducted with additional adjustments (**Supplemental Method 2**).

Using R version 3.6.1, selected findings for Model D, were presented using volcano plots (R Foundation for Statistical Computing, 2013). These plots display Log_{10}(*p*-values) for each set of models against *b* on the X-axis, highlighting findings with larger *b*. For dMRI results, these plots were presented separately for FA and MD, given their expected inverse correlation. Visualization of ROI-specific *b* with standard brain images was carried out using FSLeyes software (Jenkinson and Smith, 2001; Jenkinson et al., 2002) applied to dMRI results (URL: https://fsl.fmrib.ox.ac.uk/fsl/fslwiki/FSLeyes). Only ROIs with uncorrected *p*-value < 0.05 are presented.

RESULTS

Greater serum concentrations of 25(OH)D and folate were observed among Whites relative to AAs, with the reverse pattern observed for cobalamin. All three serum concentrations were consistently higher among "above poverty" participants (vs. below poverty), while only 25(OH)D and folate were higher in those aged >50 years at v_1 (vs. ≤50 years). Larger total and regional volumes among males, Whites, and those living above poverty (for total and GM volume) were detected compared to their counterparts ($p < 0.05$). The older group had smaller frontal GM volumes than the younger group, and differences by poverty status were mostly notable for occipital and frontal volumes (GM and WM). After multivariable adjustment, most poverty status differences in volumes became non-significant. For simplicity, only larger ROIs are presented (**Table 1**).

Top 10 adjusted associations with uncorrected $p < 0.05$ from ordinary least square brain scan-wide analyses are presented in **Tables 2–4** and **Figure 2**. Among significant findings (FWER <0.05) in the main analysis (**Table 2**), serum 25(OH)D was directly associated with larger WM volumes [overall ($\beta = +910 \pm 336$, $p = 0.007$, $q = 0.067$, passed FW Bonferroni correction), effect size $b = 0.19$], with a stronger effect size among men ($b = 0.41$). This association was specific to occipital and parietal WM, with a moderate effect size ($b = +0.23$–0.25, $q < 0.05$, passed FW Bonferroni correction) in the overall sample, men and the older group. A trend toward a direct association was also detected between 25(OH)D and total brain volume in the overall sample, in men and those in the older group. Among trends (*q*-value < 0.10), temporal and occipital WM volumes were directly associated with 25(OH)D, in Whites and individuals living above poverty, respectively. Most of these 25(OH)D vs. larger ROIs associations were not altered when additional covariates were entered in a sensitivity analysis (**Table 2**). Higher cobalamin exhibited a trend association with larger total brain, total GM, frontal and occipital GM volumes in the overall sample (*q*-value < 0.10), becoming null after adjustment for 25(OH)D and other covariates (see **Supplemental Method 2**).

For smaller ROI volumetric analysis (**Table 3**), 25(OH)D was significantly linked to larger left occipital pole volumes (FWER < 0.05, $b = +0.35$), overall and among individuals living above poverty, with a trend among men and Whites. Other stratum-specific trends were noted between 25(OH)D and right post-central gyrus volume in men, and parietal and occipital WM volume in men and the older group. Folate's relation with right temporal pole was detected among Whites ($p < 0.05$, $q < 0.10$ per vitamin, $b = -0.34$).

In the dMRI analysis (**Table 4** and **Figure 2**), both folate and 25(OH)D were significantly associated with better WMI, overall, in two key regions: Lower MD in the ALIC region for folate ($b = -0.23$, FWER < 0.05), and higher FA in the cingulum (cingulate gyrus) for 25(OH)D (FWER < 0.05, $b = +0.31$). No significant or trend associations were detected between vitamin B-12 and dMRI measures.

Figure 2 highlights the strongest effect sizes and their associated uncorrected *p*-values observed in the dMRI analysis (Model D), through a series of volcano plots applied to the overall

TABLE 1 | Study sample characteristics by sex, age group, race and poverty status; HANDLS 2004–2009 and HANDLS-SCAN 2011–2015[a].

	Total	Females	Males	≤50 years	>50 years	White	African-American	Below poverty	Above poverty
	(*N* = 240)	(*N* = 135)	(*N* = 105)	(*N* = 143)	(*N* = 97)	(*N* = 141)	(*N* = 99)	(*N* = 79)	(*N* = 161)
DEMOGRAPHIC FACTORS									
Sex, % males	41.3	—	—	41.3	47.4	44.0	43.4	35.4	47.8
Age_{v1}	47.7 ± 8.9	47.7 ± 0.8	47.9 ± 0.8	41.6 ± 0.5[c]	56.7 ± 0.4	49.0 ± 0.7[c,d]	46.1 ± 1.0	44.3 ± 0.9[c]	49.3 ± 0.7
Race, % AA	41.2	41.5	41.0	46.9[b,d]	32.0	—	—	56.6[c,d]	74.5
% above poverty	67.1	62.2	73.3	57.3[c]	81.4	74.5[3]	56.6	—	—
	(*N* = 183)	(*N* = 99)	(*N* = 84)	(*N* = 105)	(*N* = 78)	(*N* = 108)	(*N* = 75)	(*N* = 54)	(*N* = 129)
VITAMIN STATUS (v_1)									
25(OH)D, *ng/mL*	22.3 ± 10.8	20.9 ± 1.1	23.9 ± 1.1	20.5 ± 1.0[c,d]	24.7 ± 1.2	26.7 ± 1.0[c]	15.9 ± 0.9	17.2 ± 1.4[c]	24.4 ± 0.9
Median	20.0	19.0	23.0	19.0	22.5	25.5	15.0	15.5	23.0
IQR	14.0–31.0	12.0–30.0	16–32.5	12–29	16–33	19.0–34.5	10.0–19.0	9.0–21.0	16.0–33.0
% < 20	37.1	40.7	32,4	39.2	34.0	20.6[c]	60.6	48.1[c,d]	31.7
% < 10	9.6	12.6	5.7	14.0[c,d]	3.1	2.8[c]	19.2	20.3[c]	4.4
	(*N* = 240)	(*N* = 135)	(*N* = 105)	(*N* = 143)	(*N* = 97)	(*N* = 141)	(*N* = 99)	(*N* = 79)	(*N* = 161)
Serum folate, ng/mL	15.0 ± 6.3	15.0 ± 0.6	15.0 ± 0.6	13.5 ± 0.5[c]	17.4 ± 0.6	16.0 ± 0.5[c,d]	13.6 ± 0.6	13.1 ± 0.6[c]	16.1 ± 0.5
Median	14.3	14.7	14.2	12.6	17.9	15.4	12.7	12.5	15.2
IQR	9.5–20.6	9.2–20.6	9.5–20.5	8.9–17.1	12.2–22.5	10.6–21.3	8.5–17.5	8.6–17.1	10.6–21.3
% < 6	6.3	7.4	4.8	8.4	3.1	4.3	9.1	7.6	5.6
Serum B-12, *pg/mL*	518.7 ± 239.7	535.4 ± 23.0	497.2 ± 19.3	502.7 ± 18.3	542.3 ± 27.1	488.0 ± 19.7[b]	562.6 ± 24.3	475.3 ± 19.2[b]	540.0 ± 20.9
Median	463.0	464.0	456.0	460.0	464.0	438.0	521.0	455	467.0
IQR	360.0–626.5	374.0–631.0	347–623.0	359–571	362.0–644.0	339.0–571.0	390.0–679.0	338.0–457.0	364.0–644.0
% <200	0.42	—	—	—	—	—	—	—	—
BRAIN VOLUMES (v_{scan}), *mm*^{3}									
Total brain volume	970,454 ± 104,344	921,280 ± 6,311[c]	1,033,677 ± 10,198	978,724 ± 8,702	958,261 ± 10,569	989,978 ± 8,947[c]	942,645 ± 9,587	951,587 ± 11,157[b,d]	979,711 ± 8,343
Gray matter	513,545 ± 5,6152	488,776 ± 3,542[c]	545,391 ± 5,558	519,446 ± 4,752	504,846 ± 5,510	526,576 ± 4,657[c]	494,985 ± 5,249	502,325 ± 6,015[b,d]	518,559 ± 4,485
White matter	456,908 ± 51,582	432,504 ± 3,111[c]	488,286 ± 5,036	459,278 ± 4,214	453,414 ± 5,417	463,402 ± 4,531[b]	447,660 ± 4,720	448,261 ± 5,506	461,151 ± 4,134
Gray matter: Frontal	179,001 ± 20,690	170,642 ± 1,350[c]	189,748 ± 2,092	181,228 ± 1,788[b]	175,421 ± 1,947	183,082 ± 1,772[c]	173,188 ± 1890	175,430 ± 2,166[b,d]	180,752 ± 1,671
Gray matter: temporal	98,813 ± 11,598	93,343 ± 740[c]	105,847 ± 1,091	99,454 ± 982	97,869 ± 1,154	101,081 ± 956[c]	95,584 ± 1,128	96,870 ± 1255	99,767 ± 924
Gray matter: occipital	68,691 ± 9,035	65,145 ± 607[c]	73,251 ± 907	69,202 ± 765	67,937 ± 900	71,392 ± 730[c]	64,846 ± 817	66,637 ± 962[c,d]	69,699 ± 718
Gray matter: parietal	87,585 ± 11,259	83,786 ± 787[c]	92,470 ± 1,158	88,950 ± 930[b]	85,572 ± 1138	90,446 ± 926[c]	83,510 ± 1,044	85,916 ± 1,243	88,404 ± 891
White matter: Frontal	186,294 ± 21,618	176,870 ± 1,353[c]	198,412 ± 2,164	187,094 ± 1,791	185,115 ± 2,230	188,256 ± 1,888	183,500 ± 2,031	182,321 ± 2,275[b,d]	188,243 ± 1,739
White matter: temporal	104,302 ± 12,020	98,399 ± 688[c]	111,893 ± 1,181	104,782 ± 969[e]	103,596 ± 1,284	106,1044 ± 1,050[c]	101,750 ± 1,107	102,559 ± 1,268	105,158 ± 970
White matter: occipital	45,860 ± 6,113	43,155 ± 414[c]	49,338 ± 571	46,394 ± 509[e]	45,073 ± 619	46,879 ± 538[c]	44,410 ± 543	44,775 ± 627[b,d]	46,392 ± 497
White matter: parietal	90,621 ± 11,436	85,721 ± 765[c]	96,920 ± 1,101	91,074 ± 939	89,951 ± 1,193	92,253 ± 1,018[b]	88,295 ± 1,009	89,171 ± 1,270	91,332 ± 904

25(OH)D, 25-hydroxivitamin D; Age_{v1}, age measured at HANDLS visit 1 (2004–2009); HANDLS, Healthy Aging in Neighborhoods of Diversity Across the Life Span; HANDLS-SCAN, Brain magnetic resonance imaging scan ancillary study of HANDLS; IQR, Interquartile range (25th−75th percentile); v_1, visit 1 of HANDLS (2004–2009); v_{scan}, HANDLS-SCAN visit (2011–2015).

[a] *Values are Mean ± SD for totals and Mean ± SE for stratum-specific, or %. For 25(OH)D, folate and vitamin B-12, medians and inter-quartile ranges (IQR) were also provided. N = 183 for 25(OH)D analysis. The sample is that of HANDLS participants with complete visit 1 folate/B-12 measures and sMRI data [N = 240 for most analysis; N = 183 for 25(OH)D]. See methods for cutoffs chosen for each vitamin. Cobalamin deficiency analysis yielded only 1 participant below the 200 pg/mL cutoff. Thus, stratified analysis was not conducted.*

[b] *P < 0.05.*

[c] *P < 0.010 for null hypothesis of no difference by sex, age group, race, or poverty status, t-test (continuous variables), and chi-squared test (categorical variables).*

[d] *P ≥ 0.05 after adjustment for remaining covariates, multiple linear regression (continuous variables), multiple logistic regression (categorical variables).*

[e] *P < 0.05 after adjustment for remaining covariates, multiple linear regression (continuous variables), multiple logistic regression (categorical variables).*

TABLE 2 | Top 10 adjusted associations from models A (total, GM, WM) and B (regional GM, WM) vs. visit 1 exposures: serum 25(OH)D, folate and cobalamin (overall and stratified analysis) with uncorrected $P < 0.05$: ordinary least square brain scan-wide analyses on HANDLS 2004–2009 and HANDLS-SCAN 2011–2015[a].

	Outcome (v_{scan})	Outcome description	Exposure (v_1)	Stratum	(*N*)	β	(*SE*)	P_{uncorr}	Standardized Beta (b)	*q*-value	Passes FW Bonferroni correction	Standardized Beta (b): SA[b]	P_{uncorr}: SA
MODEL A													
	WM	**White matter**	**25(OH)D**	__	**(186)**	**+910**	**(336)**	**0.007**	**+0.19**	**0.067**	**Yes**	**+0.18**	**0.017**
Overall	TOTALBRAIN	Total brain volume	25(OH)D	__	(186)	+1554	(659)	0.019	+0.16	0.087[d]	No	+0.15	0.033
Stratified	**WM**	**White matter**	**25(OH)D**	**Males**	**(87)**	**+2054[c]**	**(599)**	**0.001**	**+0.41**	**0.069**	**Yes**	**+0.43**	**0.002**
	WM	White matter	25(OH)D	>50 years	(80)	+1500[c]	(470)	0.002	+0.31	0.076[d]	No	+0.25	0.017
	TOTALBRAIN	Total brain volume	25(OH)D	Males	(87)	+3537[c]	(1180)	0.004	+0.34	0.087[d]	No	+0.38	0.005
	TOTALBRAIN	Total brain volume	25(OH)D	>50 years	(80)	+2551[c]	(891)	0.005	+0.28	0.098[d]	No	+0.22	0.023
	GM	Gray matter	25(OH)D	Males	(87)	+1481	(630)	0.021	+0.26	0.29	No	+0.30	0.022
	WM	White matter	25(OH)D	AP	(132)	+930	(406)	0.024	+0.18	0.29	No	***+0.16***	***0.088***
	GM	Gray matter	25(OH)D	>50 years	(80)	+1051	(471)	0.029	+0.22	0.29	No	***+0.19***	***0.052***
	GM	Gray matter	B-12	AP	(161)	+28	(13)	0.034	+0.13	0.29	No	+0.08	0.26
	TOTALBRAIN	Total brain volume	25(OH)D	AP	(132)	+1663	(789)	0.037	+0.16	0.29	No	***+0.15***	***0.085***
	TOTALBRAIN	Total brain volume	B-12	AP	(161)	52	(26)	0.044	+0.13	0.29	No	+0.07	0.31
MODEL B													
Overall	**OCCIPITAL_WM**	**Occipital white matter**	**25(OH)D**	__	**(186)**	**+140**	**(40)**	**5.2e-04**	**+0.25**	**0.012**	**Yes**	**+0.24**	**0.001**
	PARIETAL_WM	**Parietal white matter**	**25(OH)D**	__	**(186)**	**+251**	**(77)**	**1.5e-03**	**+0.23**	**0.017**	**Yes**	**+0.22**	**0.004**
	PARIETAL_GM	Parietal gray matter	25(OH)D	__	(186)	+191	(74.9)	1.2e-02	+0.18	0.086[d]	No	+0.18	0.016
	FRONTAL_GM	Frontal gray matter	B-12	__	(240)	+11.2	(5)	1.6e-02	+0.13	0.086[d]	No	+0.07	0.27
	OCCIPITAL_GM	Occipital gray matter	B-12	__	(240)	+4.8	(2.0)	1.8e-02	+0.13	0.086[d]	No	+0.10	0.12
	TEMPORAL_WM	Temporal white matter	25(OH)D	__	(186)	+178	(77)	2.2e-02	+0.16	0.089[d]	No	+0.15	0.039
	FRONTAL_WM	Frontal white matter	25(OH)D	__	(186)	+309	(149)	3.9e-02	+0.15	0.13	No	+0.13	0.079
Stratified	**OCCIPITAL_WM**	**Occipital white matter**	**25(OH)D**	**Males**	**(87)**	**+261[c]**	**(67)**	**2.1e-04**	**+0.44**	**0.020**	**Yes**	**+0.45**	**0.001**
	PARIETAL_WM	**Parietal white matter**	**25(OH)D**	**Males**	**(87)**	**+486[c]**	**(129)**	**3.1e-04**	**+0.44**	**0.020**	**Yes**	**+0.45**	**0.001**
	OCCIPITAL_WM	**Occipital white matter**	**25(OH)D**	**>50**	**(80)**	**+205**	**(54)**	**3.2e-04**	**+0.37**	**0.020**	**Yes**	**+0.27**	**0.005**
	PARIETAL_WM	**Parietal white matter**	**25(OH)D**	**>50**	**(80)**	**+393[c]**	**(108)**	**5.4e-04**	**+0.37**	**0.020**	**Yes**	**+0.32**	**0.004**
	OCCIPITAL_WM	Occipital white matter	25(OH)D	AP	(132)	+156	(48)	1.3e-03	+0.25	0.050[d]	No	+0.26	0.004
	OCCIPITAL_WM	Occipital white matter	25(OH)D	Whites	(109)	+155	(49)	2.2e-03	+0.25	0.063[d]	No	+0.28	0.002
	FRONTAL_WM	Frontal white matter	25(OH)D	Males	(87)	+826[c]	(262)	2.3e-03	+0.38	0.063[d]	No	+0.42	0.003
	TEMPORAL_WM	Temporal white matter	25(OH)D	>50	(80)	+326[c]	(108)	3.5e-03	+0.29	0.084[d]	No	+0.23	0.024
	TEMPORAL_GM	Temporal gray matter	FOL	Whites	(109)	−354[c]	(123)	4.7e-03	−0.20	0.10	No	−0.26	0.004
	FRONTAL_GM	Fontal gray matter	B-12	AP	(132)	+13.4	(5.1)	9.7e-03	+0.17	0.18	No	+0.09	0.22

25(OH)D, 25-hydroxyvitamin D; AP, Above poverty; B-12, serum cobalamin (vitamin B-12); FDR, False Discovery Rate; FOL, serum folate; FWER, FamilyWise Error Rate; GM, Gray Matter; SA, Sensitivity Analysis; SE, Standard Error; WM, White Matter.

[a] *Values are adjusted linear regression coefficients β with associated SE, standardized beta, uncorrected p-values, corrected q-values (false discovery rate) and results of sensitivity analysis. (N) is the sample size in each analysis. Bolded rows correspond to statistically significant associations after correction for multiple testing, FWER < 0.05.*

[b] *Based on a sensitivity analysis further adjusting for selected socio-demographic, lifestyle and health-related factors after screening using machine learning techniques (see* ***Supplemental Methods 2****). Note that for visit 1 25(OH)D, no additional covariates were selected. For Folate and B-12 a reduced set of additional covariates were included and are listed in* ***Supplemental Methods 2****.*

[c] *$P < 0.10$ for null hypothesis that exposure×stratifying variable 2-way interaction term is =0 in the unstratified model with exposure and socio-demographic factors included as main effects.*

[d] *Finding considered a trend for passing FDR q-value correction at type I error of 0.10 per vitamin, model and stratification status while failing the FWER criterion, due to a standardized effect size (in absolute value) ≥0.20.*

TABLE 3 | Top 10 adjusted associations from model C, small sMRI regions vs. visit 1 exposures: serum 25(OH)D, folate and cobalamin (overall and stratified analysis) with uncorrected $P < 0.05$: ordinary least square brain scan-wide analyses on HANDLS 2004–2009 and HANDLS-SCAN 2011–2015[a].

Outcome (v_{scan})	Outcome description	Exposure (v_1)	Stratum	(*N*)	β	(*SE*)	*P*	Standardized Beta (b)	*q*-value	Passes FW Bonferroni correction	Standardized Beta (b): SA[b]	P_{uncorr}: SA
OVERALL												
Left_OCP_occipital_pole	**Left occipital pole**	**25(OH)D**	__	**(186)**	**+15.70**	**(3.83)**	**6.3e-05**	**+0.31**	**0.026**	**Yes**	**+0.27**	**<0.001**
occipital_lobe_WM_left	Occipital lobe, white matter, left	25(OH)D	__	(186)	+76.8	(20.7)	2.9e-04	+0.26	0.061[d]	No	+0.26	<0.001
Right_PoG_post-central_gyrus	Post-central gyrus, right	25(OH)D	__	(186)	+34.8	(9.7)	4.3e-04	+0.27	0.061[d]	No	+0.27	0.001
parietal_lobe_WM_right	Parietal lobe, white matter, right	25(OH)D	__	(186)	+127.9	(38.1)	9.8e-04	+0.24	0.10[d]	No	+0.23	0.002
Left_PoG_post-central_gyrus	Post-central gyrus, left	25(OH)D	__	(186)	+34.1	(10.4)	1.3e-03	+0.25	0.11[d]	No	+0.25	0.002
Right_TrIFG_triangular_part_of_t	Triangular part of the inferior frontal gyrus, right	B-12	__	(240)	+0.45	(0.14)	2.2e-03	+0.20	0.13	No	+0.19	0.017
parietal_lobe_WM_left	Parietal lobe, white matter, left	25(OH)D	__	(186)	+123.4	(40.4)	3.1e-03	+0.22	0.13[d]	No	+0.21	0.007
occipital_lobe_WM_right	Occipital lobe, white matter, right	25(OH)D	__	(186)	+63.6	(21.1)	3.0e-03	+0.21	0.13[d]	No	+0.21	0.005
Right_TMP_temporal_pole	Right temporal pole	FOL	__	(240)	−35.5	(11.9)	2.7e-03	−0.19	0.13	No	−0.22	0.010
Anterior insula, right	Right_AIns_anterior_insula	B-12	__	(240)	+0.36	(0.12)	3.2e-03	+0.17	0.13	No	+0.13	0.071
STRATIFIED												
Left_OCP_occipital_pole	**Left occipital pole**	**25(OH)D**	**AP**	**(132)**	**+19.0[c]**	**(4.3)**	**2.0e-05**	**+0.35**	**0.07**	**Yes**	**+0.32**	**<0.001**
Right_TMP_temporal_pole	Right temporal pole	FOL	Whites	(141)	−63.9[c]	(15.2)	4.8e-05	−0.34	0.08[d]	No	−0.42	<0.001
Left_OCP_occipital_pole	Left occipital pole	25(OH)D	Men	(87)	+24.0	(5.8)	8.0e-05	+0.45	0.09[d]	No	+0.46	<0.001
Left_OCP_occipital_pole	Left occipital pole	25(OH)D	Whites	(109)	+17.7	(4.5)	1.6e-04	+0.33	0.11[d]	No	+0.31	0.001
Right_PoG_post-central_gyrus	Right post-central gyrus	25(OH)D	Men	(87)	+64.4[c]	(16.6)	1.6e-04	+0.43	0.13[d]	No	+0.47	0.001
Parietal_lobe_WM_right	Right parietal lobe, White matter	25(OH)D	Men	(87)	+242.6[c]	(63.4)	2.6e-04	+0.45	0.13[d]	No	+0.46	0.001
occipital_lobe_WM_left	Occipital lobe, white matter, left	25(OH)D	>50	(80)	+107.7	(28.0)	3.4e-04	+0.37	0.14[d]	No	+0.28	0.004
parietal_lobe_WM_left	Parietal lobe, white matter, left	25(OH)D	>50	(80)	+201.8[c]	(53.6)	3.4e-04	+0.39	0.14[d]	No	+0.34	0.003
occipital_lobe_WM_right	Occipital lobe, white matter, right	25(OH)D	Men	(87)	+132.3[c]	(35.9)	4.1e-04	+0.43	0.14[d]	No	+0.44	0.001
Right_PHG_parahippocampal_gyrus	Right parahippocampal gyrus	FOL	Whites	(141)	−20.6[c]	(5.7)	4.2e-04	−0.27	0.14	No	−0.38	<0.001

25(OH)D, 25-hydroxyvitamin D; AP, Above poverty; B-12, serum cobalamin (vitamin B-12); FDR, False Discovery Rate; FOL, serum folate; FWER, FamilyWise Error Rate; GM, Gray Matter; SA, Sensitivity Analysis; SE, Standard Error; WM, White Matter.

[a] *Values are adjusted linear regression coefficients β with associated SE, standardized beta, uncorrected p-values, corrected q-values (false discovery rate) and results of sensitivity analysis. (N) is the sample size in each analysis. Bolded rows correspond to statistically significant associations after correction for multiple testing, FWER < 0.05.*

[b] *Based on a sensitivity analysis further adjusting for selected socio-demographic, lifestyle and health-related factors after screening using machine learning techniques (see **Supplemental Methods 2**). Note that for visit 1 25(OH)D, no additional covariates were selected. For Folate and B-12 a reduced set of additional covariates were included and are listed in **Supplemental Methods 2**.*

[c] *P<0.10 for null hypothesis that exposure × stratifying variable 2-way interaction term is =0 in the unstratified model with exposure and socio-demographic factors included as main effects.*

[d] *Finding considered a trend for passing FDR q-value correction at type I error of 0.10 per vitamin, model and stratification status while failing the FWER criterion, due to a standardized effect size (in absolute value) ≥0.20.*

TABLE 4 | Top 10 adjusted associations from model D, bilateral means of MD and FA from dMRI vs. visit 1 exposures: serum 25(OH)D, folate and cobalamin (overall and stratified analysis) with uncorrected $P < 0.05$: ordinary least square brain scan-wide analyses on HANDLS 2004–2009 and HANDLS-SCAN 2011–2015[a].

Outcome (v_{scan})	Outcome description	Exposure (v_1)	Stratum	(*N*)	β	(*SE*)	*P*	Standardized Beta (b)	*q*-value	Passes FW Bonferroni correction	Standardized Beta (b): SA[b]	P_{uncorr}: SA
OVERALL												
alic_b_tr	**Anterior limb of the internal capsule, Mean diffusivity, bilateral mean**	**FOL**	__	**(240)**	**−5.64e-06**	**(1.56e-06)**	**3.8e-04**	**−0.23**	**0.074[d]**	**Yes**	**−0.26**	**0.003**
cgc_b_fa	**Cingulum (Cingulate Gyrus), fractional anisotropy, bilateral mean**	**25(OH)D**	__	**(185)**	**+0.0007**	**(0.0002)**	**4.1e-04**	**+0.31**	**0.074[d]**	**Yes**	**+0.28**	**0.002**
alic_b_fa	Anterior limb of the internal capsule, fractional anisotropy, bilateral mean	25(OH)D	__	(185)	+0.0006	(0.0002)	9.7e-04	+0.29	0.12[d]	No	+0.22	0.005
mcp_b_tr	Middle cerebellar peduncle, mean diffusivity, bilateral mean	B-12	__	(240)	−1.45e-07	(4.81e-08)	2.8e-03	−0.19	0.22	No	−0.18	0.019
mfowm_b_tr	Middle Fronto-Orbital WM, mean diffusivity, bilateral mean	FOL	__	(240)	−5.68e-06	(1.93e-06)	3.7e-03	−0.19	0.22	No	−0.23	0.019
cgh_b_fa	Cingulum (Hippocampus), fractional anisotropy, bilateral mean	25(OH)D	__	(185)	+0.0006	(0.0002)	3.9e-03	+0.25	0.22	No	+0.21	0.023
icp_b_fa	Inferior cerebellar peduncle, fractional anisotropy, bilateral mean	FOL	__	(240)	+0.0009	(0.0003)	4.5e-03	+0.19	0.22	No	+0.22	0.015
ss_b_fa	Sagittal Stratum, fraction anisotropy, bilateral mean	25(OH)D	__	(185)	+0.0004	(0.0002)	4.9e-03	+0.25	0.22	No	+0.20	0.010
mowm_b_tr	Middle Occipital WM, mean diffusivity, bilateral mean	FOL	__	(240)	−4.13e-06	(1.50e-06)	6.5e-03	−0.18	0.22	No	−0.17	0.024
put_b_tr	Putamen, mean diffusivity, bilateral mean	FOL	__	(240)	−4.22e-06	(1.54e-06)	6.5e-03	−0.18	0.22	No	−0.26	0.004
STRATIFIED												
alic_b_fa	Anterior limb of the internal capsule, fractional anisotropy, bilateral mean	25(OH)D	Whites	(109)	+0.0009[c]	(0.0002)	8.6e-05	+0.37	0.11[d]	No	+0.32	0.001
bcc_b_tr	Body of corpus callosum, Mean diffusivity, bilateral mean	25(OH)D	BP	(52)	−0.00002[c]	(4.43e-06)	8.7e-05	−0.53	0.11[d]	No	−0.61	0.001
cgc_b_fa	Cingulum (Cingulate Gyrus), fractional anisotropy, bilateral mean	25(OH)D	Whites	(109)	+0.0008	(0.0002)	1.1e-04	+0.39	0.11[d]	No	+0.36	<0.001
sowm_b_fa	Superior Occipital WM, fractional anisotropy, bilateral mean	FOL	Males	(103)	+0.0016[c]	(0.0004)	2.1e-04	+0.39	0.12[d]	No	+0.31	0.007
unc_b_tr	Uncinate Fasciculus, mean diffusivity, bilateral mean	FOL	AA	(98)	2.2e-04[c]	(2.33e-06)	3.4e-04	−0.40	0.12[d]	No	−0.39	0.004
alic_b_tr	Anterior limb of the internal capsule, Mean diffusivity, bilateral mean	FOL	AP	(163)	−6.44e-06	1.72e-06	4.6e-04	−0.27	0.12[d]	No	−0.30	0.004
scc_b_tr	Splenium of Corpus Callosum, Mean diffusivity, bilateral mean	25(OH)D	BP	(52)	−0.000015[c]	(3.80e-06)	3.0e-04	−0.50	0.12[d]	No	−0.63	0.001
sowm_b_tr	Superior Occipital WM, mean diffusivity, bilateral mean	FOL	Males	(103)	−0.00001[c]	(3.53e-06)	4.6e-04	−0.37	0.15[d]	No	−0.38	<0.001
alic_b_tr	Anterior limb of the internal capsule, Mean diffusivity, bilateral mean	FOL	>50 years	(96)	−0.00001[c]	(2.92e-06)	2.8e-04	−0.36	0.15[d]	No	−0.44	0.011
cgc_b_fa	Cingulum (Cingulate Gyrus), fractional anisotropy, bilateral mean	25(OH)D	BP	(52)	+0.00150	0.00040	5.8e-04	+0.57	0.17[d]	No	+0.59	0.003

25(OH)D, 25-hydroxyvitamin D; AP, Above poverty; B-12, serum cobalamin (vitamin B-12); FOL, serum folate; FWER, FamilyWise Error Rate; GM, Gray Matter; SA, Sensitivity Analysis; SE, Standard Error; WM, White Matter.

[a]Values are adjusted linear regression coefficients β with associated SE, standardized beta, uncorrected p-values, corrected q-values (false discovery rate) and results of sensitivity analysis. (N) is the sample size in each analysis. Bolded rows correspond to statistically significant associations after correction for multiple testing, FWER < 0.05.

*[b]Based on a sensitivity analysis further adjusting for selected socio-demographic, lifestyle and health-related factors after screening using machine learning techniques (see **Supplemental Methods 2**). Note that for visit 1 25(OH)D, no additional covariates were selected. For Folate and B-12 a reduced set of additional covariates were included and are listed in **Supplemental Methods 2**.*

[c]$P < 0.10$ for null hypothesis that exposure × stratifying variable 2-way interaction term is =0 in the unstratified model with exposure and socio-demographic factors included as main effects.

[d]Finding considered a trend for passing FDR q-value correction at type I error of 0.10 per vitamin, model and stratification status while failing the FWER criterion, due to a standardized effect size (in absolute value) ≥0.20.

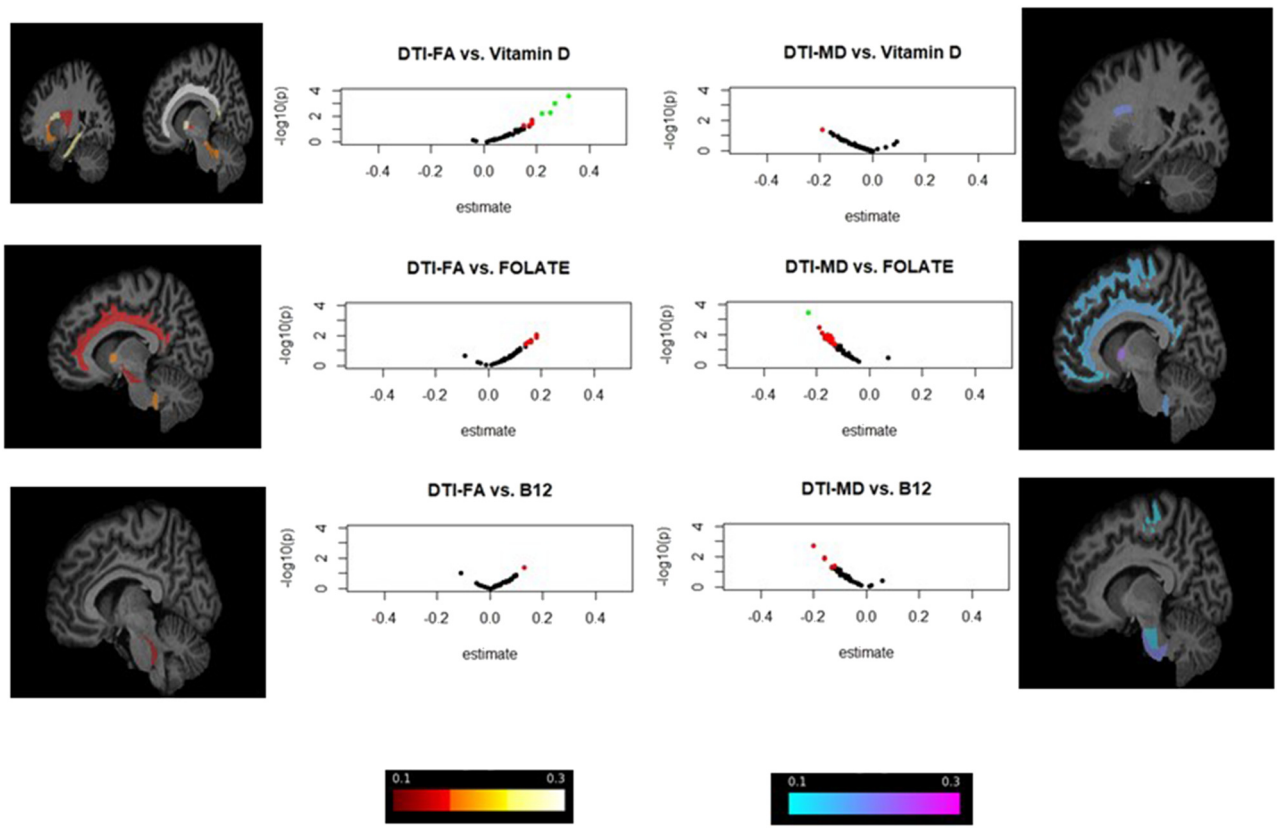

FIGURE 2 | ROI-wide brain dMRI association with v_1 serum 25(OH)D, folate and cobalamin in total population: volcano plots and brain image visualization for HANDLS 2004–2009 and HANDLS-SCAN 2011–2015[a,b]. [a]Volcano plots display Log_{10}(*p*-values) for each set of models against the standardized effect (b) on the X-axis, highlighting findings with larger effect sizes. Associations with $P < 0.05$ are presented in red, whereas those with both $P < 0.05$ and effect size in absolute value >0.20 are presented in green. [b]Brain visualization using FSLeyes program is focused on standardized effect sizes (b) and direction, with negative effects ($b < 0$) shown in cold colors and positive effects ($b > 0$) shown in warmer colors. The range is between −0.3 and +0.3 with lighter colors indicating stronger effects in either direction. Only ROIs with uncorrected *p*-value < 0.05 are presented.

study sample, applied to v_1 exposures. Effect sizes and direction were also visualized on standard ROI-specific brain images, for associations with $p_{uncorr} < 0.05$.

DISCUSSION

This study is among few that used a brain scan-wide analysis methodology to test associations of serum 25(OH)D, folate and cobalamin with brain volumes and WMI and the first to do so among socio-demographically diverse adults. The 3 vitamin status measures were systematically correlated with sMRI/dMRI brain markers, from low-to-high segmentation levels. We found statistically significant (FWER < 0.05) direct associations of 25(OH)D(v_1) with total, occipital and parietal WM volumes, particularly among men and older participants and with left occipital pole volume, overall and among individuals living above poverty. Only trends were detected for cobalamin exposures ($q < 0.10$), while serum folate (v_1) were associated with lower mean diffusivity (MD) in ALIC and with fractional anisotropy in the cingulum (cingulate gyrus), respectively, reflecting greater WMI, overall.

In terms of 25(OH)D and sMRI markers, vitamin D deficiency appears to be associated with smaller hippocampal subfields in MCI participants (Karakis et al., 2016; Al-Amin et al., 2019). Our study indicated that 25(OH)D was inversely linked to WM volumes, particularly in the left occipital pole. The occipital pole encompasses the primary visual cortex and contributes to language abilities (Charles et al., 1997; Melrose et al., 2009). Decline in verbal fluency has been related to lower 25(OH)D status (Beydoun et al., 2018; Goodwill et al., 2018). Relations of vitamin D deficiency with smaller WM volumes and poorer integrity were shown elsewhere (Buell et al., 2010; Prager et al., 2014; Annweiler et al., 2015b; Del Brutto et al., 2015). Vitamin D status was also associated with larger GM volumes (Brouwer-Brolsma et al., 2015), smaller ventricles (Annweiler et al., 2013) or not related to brain markers (Michos et al., 2014; Littlejohns et al., 2016). Our race-specific associations are notable, possibly due to genetic polymorphisms determining brain vitamin D status, which pending further studies, may be higher among Whites compared to AAs (Powe et al., 2013; Berg et al., 2015).

Among comparable ROI-specific dMRI studies, a cross-sectional study (Moon et al., 2015), found an inverse association

between 25(OH)D and FA values near the inferior and superior longitudinal fasciculi, corpus callosum (genu), the anterior corona radiata, the ALIC and the cingulum bundle. Most regional FAs, particularly the ALIC and cingulum bundle (cingulate and hippocampus), were found to be positively associated with 25(OH)D in our study, with the cingulate gyrus exhibiting statistical significance.

Similarly, folate and cobalamin were previously linked to larger brain volumes (or slower atrophy), specifically within hippocampal and amygdala regions (Scott et al., 2004; Vogiatzoglou et al., 2008; Lee et al., 2016) and reduced WM lesion severity (De Lau et al., 2009; Pieters et al., 2009). In our study, cobalamin was related to occipital and temporal GM volumes, an association that was attenuated with full covariate-adjustment. B-6 and cobalamin intakes were also shown to spare GM atrophy, with specific association between cobalamin status and bi-lateral superior parietal sulcus (Erickson et al., 2008). Moreover, direct relationship between cobalamin status and regional GM volume (right precuneus, right post-central gyrus and left inferior parietal lobule) in AD was found mostly among ApoE4+ individuals (Lee et al., 2016). Our study showed a trend between increasing levels of cobalamin and larger parts of the inferior frontal gyrus [orbital (left); triangular (right)], known for its function in processing speech and language (Greenlee et al., 2007). A longitudinal study of adults found that lower cobalamin status, but not folate, was linked to increased rate of brain volume loss. A recent trial (VITACOG) conducted among MCI patients showed that GM regions vulnerable to AD, such as the medial temporal lobe, benefited from high-dose B vitamin supplementation by slowing atrophy rates over 2 years, though this pertained only to hyperhomocysteinemic individuals (Douaud et al., 2013), and this trial indicated that B vitamin supplementation can stabilize executive functions and reduce decline in global cognition, episodic and semantic memory (De Jager et al., 2012).

Novel are our findings that folate and 25(OH)D are related to greater white matter integrity, with folate being inversely related to MD in the ALIC region while 25(OH)D being related to higher FA in the cingulum (cingulate gyrus). While previous studies have linked vitamin D and folate deficiency to WM damage (Sachdev et al., 2002; Bleich and Kornhuber, 2003; Den Heijer et al., 2003; Dufouil et al., 2003; Scott et al., 2004; Censori et al., 2007; De Lau et al., 2009; Pieters et al., 2009; Buell et al., 2010; Prager et al., 2014; Annweiler et al., 2015b; Del Brutto et al., 2015; Moon et al., 2015; Wu et al., 2015; Lee et al., 2017), our study further specified most affected ROIs and target socio-demographic groups. The ALIC connects the thalamus with the frontal lobe, suggesting these nutrients can maintain cognitive functions that are reliant on frontothalamic connectivity, such as executive function (Schoenberg and Scott, 2011; Jacobs et al., 2013). Despite folate not being consistently associated with executive function or attention (Rosenberg, 2008), it was inversely related to depression (Bender et al., 2017) and reduced ALIC FA prevails in depressive disorders (Zou et al., 2008; Jia et al., 2010; Chen et al., 2016). Moreover, depressive symptoms increase dementia risk (Tan et al., 2019). Thus, future studies could explore mediation of the depression-AD relationship through ALIC FA and MD as the mechanism for folate supplementation prevention.

Our findings indicate that in certain sub-groups, folate may adversely affect volumetric markers, specifically the right temporal pole volume, thought to contribute to personal and episodic memories, also shown to be linked with empathy (Rankin et al., 2006). The literature shows an interaction between folate and cobalamin status, whereby high folate status coupled with cobalamin deficiency was associated with smaller GM volumes in the right middle occipital gyrus and the opercular part of the inferior frontal gyrus (Deng et al., 2017). Thus, abnormally high levels of folate may relate to poorer outcomes, though this finding may be spurious and due to chance, requiring replication in a larger meta-analytic studies.

Our study has several notable strengths. First, it examined the association between several AD-related nutritional biomarkers with brain structural sMRI and dMRI measures reflecting regional volumes and WMI, potentially underlying various neuropathologies. Moreover, while cross-sectional, this study provided 5–6 years of latency between exposure (nutritional biomarkers) and outcome (brain MRI measures) and secondarily tested stratum-specific heterogeneity and adjusting for multiple testing. Additionally, given that serum 25(OH)D was recently linked to lower intracranial volume (ICV) (Annweiler et al., 2015a), our detected positive association between 25(OH)D and brain volumes, including WM, may be conservative and under-estimated, and may be inflated upon ICV adjustment.

Nevertheless, study findings should be interpreted with caution given limitations. First, due to dMRI voxel size limitations, partial volume effects and possible contamination by nearby cerebral spinal fluid can occur, increasing FA and MD estimation errors. Second, timing of blood sample collection and measurement errors may have affected the sample distribution of serum 25(OH)D levels, with overestimation as a possibility as 10%-15% of the measured 25(OH)D values are in fact 24,25-dihydroxyvitamin D, which is recognized by the same antibody. Third, the latency between exposure and outcome could make the findings somewhat speculative when compared to a cohort study whereby baseline exposure is being tested against annualized change in outcome. The lack of a baseline sMRI/dMRI measure is a notable limitation of this study that should be remedied in further studies of comparable populations. Other potential limitations include the lack of other related serum measures, such as Hcy and vitamin B-6 in HANDLS, the lack of longer term markers, such as red blood cell folate, residual confounding particularly by physical activity which was not adequately measured at v_1, non-participation selection bias, and a lower powered stratum-specific associations especially by race and poverty status. Due to differences in dietary intakes, absorption, utilization, distribution or other confounding conditions, circulating levels of target vitamins may not reflect their brain tissue levels, reducing their value as biomarkers. Moreover, our strongest findings implicate 25(OH)D as the main exposure, which may confound the association of serum folate with region-specific WMI. A

larger meta-analytic study may be needed to disentangle those associations. Finally, external validity may be limited to inner US cities with similar racial/ethnic and socio-economic diversity as Baltimore City, as well as to middle-aged adults.

In summary, serum 25(OH)D status was consistently linked to larger occipital and parietal WM volumes and regional WMI. Pending longitudinal replication of our findings, future interventions should test vitamin D supplementation against regional volumetric and diffusion brain markers and mechanistic studies are needed to examine regional vulnerability to vitamin status.

DATA AVAILABILITY STATEMENT

Data are available upon request to researchers with valid proposals who agree to the confidentiality agreement as required by our Institutional Review Board. We publicize our policies on our website https://handls.nih.gov, which contains the code book for the parent study, HANDLS. Requests for data access may be sent to the PIs or the study manager, Jennifer Norbeck at norbeckje@mail.nih.gov. These data are owned by the National Institute on Aging at the National Institutes of Health. The Principal Investigators, have restricted public access to these data because (1) the study collects medical, psychological, cognitive, and psychosocial information on racial and poverty differences that could be misconstrued or willfully manipulated to promote racial discrimination; and (2) although the sample is fairly large, there are sufficient identifiers that the PIs cannot guarantee absolute confidentiality for every participant as we have stated in acquiring our confidentiality certificate. Analytic scripts and code book specific to HANDLS-SCAN can be obtained from the corresponding author upon request.

ETHICS STATEMENT

The studies involving human participants were reviewed and approved by National Institute on Environmental Health Sciences IRB committee. The patients/participants provided their written informed consent to participate in this study.

AUTHOR CONTRIBUTIONS

MB contributed to the study concept, planned the analysis, conducted the data management and statistical analysis, conducted the literature review, wrote and revised the manuscript. DS planned the analysis, conducted the data management, conducted the literature review, wrote and revised the parts of the manuscript. SH conducted the literature search and review, assisted in statistical analysis, wrote the parts of the manuscript, and revised the manuscript. HB planned the analysis, conducted the literature review, wrote the parts of the manuscript, and revised the manuscript. LK, CD, RG, SS, and ME acquired the data, wrote and revised the parts of the manuscript. GE acquired the data, planned the analysis, assisted in data management and statistical analysis, wrote and revised the parts of the manuscript. AZ and SW acquired the data, the planned analysis, wrote and revised the parts of the manuscript.

FUNDING

This work was supported in part by the Intramural research Program of the NIH, National institute on Aging. This work was also supported by the National Institutes of Health, R01-AG034161 to SW, ZIA–AG000513 to ME and AZ, and The University of Maryland Claude D. Pepper Older Americans Independence Center (NIH grant P30 AG028747).

ACKNOWLEDGMENTS

We would like to thank Ms. Megan Williams and Ms. Nicolle Mode (NIA/NIH/IRP) for internally reviewing our manuscript. We acknowledge the Core for Translational Research in Imaging @ Maryland (CTRIM) which is a part of the University of Maryland School of Medicine Center for Innovative Biomedical Resources- Baltimore, Maryland.

SUPPLEMENTARY MATERIAL

The Supplementary Material for this article can be found online at: https://www.frontiersin.org/articles/10.3389/fnagi.2020.00140/full#supplementary-material

REFERENCES

Al-Amin, M., Bradford, D., Sullivan, R. K. P., Kurniawan, N. D., Moon, Y., Han, S. H., et al. (2019). Vitamin D deficiency is associated with reduced hippocampal volume and disrupted structural connectivity in patients with mild cognitive impairment. *Hum. Brain Mapp.* 40, 394–406. doi: 10.1002/hbm.24380

Annweiler, C., Bartha, R., Goncalves, S., Karras, S. N., Millet, P., Feron, F., et al. (2015a). Vitamin D-related changes in intracranial volume in older adults: a quantitative neuroimaging study. *Maturitas* 80, 312–317. doi: 10.1016/j.maturitas.2014.12.011

Annweiler, C., Bartha, R., Karras, S. N., Gautier, J., Roche, F., and Beauchet, O. (2015b). Vitamin D and white matter abnormalities in older adults: a quantitative volumetric analysis of brain MRI. *Exp. Gerontol.* 63, 41–47. doi: 10.1016/j.exger.2015.01.049

Annweiler, C., Milea, D., Whitson, H. E., Cheng, C. Y., Wong, T. Y., Ikram, M. K., et al. (2016). Vitamin D insufficiency and cognitive impairment in Asians: a multi-ethnic population-based study and meta-analysis. *J. Intern. Med.* 280, 300–311. doi: 10.1111/joim.12491

Annweiler, C., Montero-Odasso, M., Hachinski, V., Seshadri, S., Bartha, R., and Beauchet, O. (2013). Vitamin D concentration and lateral cerebral ventricle volume in older adults. *Mol. Nutr. Food Res.* 57, 267–276. doi: 10.1002/mnfr.201200418

Bender, A., Hagan, K. E., and Kingston, N. (2017). The association of folate and depression: a meta-analysis. *J. Psychiatr. Res.* 95, 9–18. doi: 10.1016/j.jpsychires.2017.07.019

Berg, A. H., Powe, C. E., Evans, M. K., Wenger, J., Ortiz, G., Zonderman, A. B., et al. (2015). 24,25-Dihydroxyvitamin d3 and vitamin D status of community-dwelling black and white Americans. *Clin. Chem.* 61, 877–884. doi: 10.1373/clinchem.2015.240051

Beydoun, M. A., Beydoun, H. A., Gamaldo, A. A., Teel, A., Zonderman, A. B., and Wang, Y. (2014a). Epidemiologic studies of modifiable factors associated with cognition and dementia: systematic review and meta-analysis. *BMC Public Health* 14:643. doi: 10.1186/1471-2458-14-643

Beydoun, M. A., Fanelli Kuczmarski, M. T., Beydoun, H. A., Shroff, M. R., Mason, M. A., Evans, M. K., et al. (2010a). The sex-specific role of plasma folate in mediating the association of dietary quality with depressive symptoms. *J. Nutr.* 140, 338–347. doi: 10.3945/jn.109.113878

Beydoun, M. A., Gamaldo, A. A., Canas, J. A., Beydoun, H. A., Shah, M. T., Mcneely, J. M., et al. (2014b). Serum nutritional biomarkers and their associations with sleep among US adults in recent national surveys. *PLoS ONE* 9:e103490. doi: 10.1371/journal.pone.0103490

Beydoun, M. A., Hossain, S., Fanelli-Kuczmarski, M. T., Beydoun, H. A., Canas, J. A., Evans, M. K., et al. (2018). Vitamin D status and intakes and their association with cognitive trajectory in a longitudinal study of urban adults. *J. Clin. Endocrinol. Metab.* 103, 1654–1668. doi: 10.1210/jc.2017-02462

Beydoun, M. A., Shroff, M. R., Beydoun, H. A., and Zonderman, A. B. (2010b). Serum folate, vitamin B-12, and homocysteine and their association with depressive symptoms among U.S. *adults. Psychosom. Med.* 72, 862–873. doi: 10.1097/PSY.0b013e3181f61863

Bleich, S., and Kornhuber, J. (2003). Relationship between plasma homocysteine levels and brain atrophy in healthy elderly individuals. *Neurology 60, 1539–1541*. doi: 10.1212/WNL.60.7.1220

Bottiglieri, T. (2005). Homocysteine and folate metabolism in depression. *Prog. Neuropsychopharmacol. Biol. Psychiatry* 29, 1103–12. doi: 10.1016/j.pnpbp.2005.06.021

Brouwer-Brolsma, E. M., Van Der Zwaluw, N. L., Van Wijngaarden, J. P., Dhonukshe-Rutten, R. A., In 'T Veld, P. H., Feskens, E. J., et al. (2015). Higher serum 25-hydroxyvitamin D and lower plasma glucose are associated with larger gray matter volume but not with white matter or total brain volume in Dutch community-dwelling older adults. *J. Nutr.* 145, 1817–1823. doi: 10.3945/jn.115.214197

Buell, J. S., and Dawson-Hughes, B. (2008). Vitamin D and neurocognitive dysfunction: preventing "D"ecline? *Mol. Aspects Med.* 29, 415–422. doi: 10.1016/j.mam.2008.05.001

Buell, J. S., Dawson-Hughes, B., Scott, T. M., Weiner, D. E., Dallal, G. E., Qui, W. Q., et al. (2010). 25-Hydroxyvitamin D, dementia, and cerebrovascular pathology in elders receiving home services. *Neurology* 74, 18–26. doi: 10.1212/WNL.0b013e3181beecb7

Carro, E., Spuch, C., Trejo, J. L., Antequera, D., and Torres-Aleman, I. (2005). Choroid plexus megalin is involved in neuroprotection by serum insulin-like growth factor I. *J. Neurosci.* 25, 10884–10893. doi: 10.1523/JNEUROSCI.2909-05.2005

Censori, B., Partziguian, T., Manara, O., and Poloni, M. (2007). Plasma homocysteine and severe white matter disease. *Neurol. Sci.* 28, 259–263. doi: 10.1007/s10072-007-0832-y

Centers for Disease Control and Prevention (2006). *25-Hydroxyvitamin D in Serum*, (Hyattsville, MD).

Charles, P. D., Abou-Khalil, B., Atkinson, D. S. Jr., Bakar, M., Mayville, C. L., and Kirshner, H. S. (1997). Occipital pole area and language dominance. *J. Neuroimaging* 7, 89–91. doi: 10.1111/jon19977289

Chen, G., Hu, X., Li, L., Huang, X., Lui, S., Kuang, W., et al. (2016). Disorganization of white matter architecture in major depressive disorder: a meta-analysis of diffusion tensor imaging with tract-based spatial statistics. *Sci. Rep.* 6:21825. doi: 10.1038/srep21825

De Jager, C. A., Oulhaj, A., Jacoby, R., Refsum, H., and Smith, A. D. (2012). Cognitive and clinical outcomes of homocysteine-lowering B-vitamin treatment in mild cognitive impairment: a randomized controlled trial. *Int. J. Geriatr. Psychiatry* 27, 592–600. doi: 10.1002/gps.2758

De Lau, L. M., Smith, A. D., Refsum, H., Johnston, C., and Breteler, M. M. (2009). Plasma vitamin B12 status and cerebral white-matter lesions. *J. Neurol. Neurosurg. Psychiatry* 80, 149–157. doi: 10.1136/jnnp.2008.149286

Deane, R., Wu, Z., Sagare, A., Davis, J., Du Yan, S., Hamm, K., et al. (2004). LRP/amyloid beta-peptide interaction mediates differential brain efflux of Abeta isoforms. *Neuron* 43, 333–344. doi: 10.1016/j.neuron.2004.07.017

Del Brutto, O. H., Mera, R. M., Macias, J., Morales, G., and Zambrano, M. (2015). Cerebrovascular correlates of vitamin D deficiency in older adults living near the equator: results from the atahualpa project. *Int. J. Stroke* 10, 1301–1303. doi: 10.1111/ijs.12627

Den Heijer, T., Vermeer, S. E., Clarke, R., Oudkerk, M., Koudstaal, P. J., Hofman, A., et al. (2003). Homocysteine and brain atrophy on MRI of non-demented elderly. *Brain* 126, 170–175. doi: 10.1093/brain/awg006

Deng, Y., Wang, D., Wang, K., and Kwok, T. (2017). High serum folate is associated with brain atrophy in older diabetic people with vitamin B12 deficiency. *J. Nutr. Health Aging* 21, 1065–1071. doi: 10.1007/s12603-017-0979-z

Diagnostics, Q. (2019). *Vitamin D, 25-Hydroxy, Total, Immunoassay. Available online at:* https://testdirectory.questdiagnostics.com/test/test-detail/17306/vitamin-d-25-hydroxy-total-immunoassay?cc=MASTER (accessed December 16, 2019).

Douaud, G., Refsum, H., De Jager, C. A., Jacoby, R., Nichols, T. E., Smith, S. M., et al. (2013). Preventing Alzheimer's disease-related gray matter atrophy by B-vitamin treatment. *Proc. Natl. Acad. Sci. U.S.A.* 110, 9523–9528. doi: 10.1073/pnas.1301816110

Dufouil, C., Alperovitch, A., Ducros, V., and Tzourio, C. (2003). Homocysteine, white matter hyperintensities, and cognition in healthy elderly people. *Ann. Neurol.* 53, 214–221. doi: 10.1002/ana.10440

Erickson, K. I., Suever, B. L., Prakash, R. S., Colcombe, S. J., Mcauley, E., and Kramer, A. F. (2008). Greater intake of vitamins B6 and B12 spares gray matter in healthy elderly: a voxel-based morphometry study. *Brain Res.* 1199, 20–26. doi: 10.1016/j.brainres.2008.01.030

Etgen, T., Sander, D., Bickel, H., Sander, K., and Forstl, H. (2012). Vitamin D deficiency, cognitive impairment and dementia: a systematic review and meta-analysis. *Dement. Geriatr. Cogn. Disord.* 33, 297–305. doi: 10.1159/000339702

Evans, M. K., Lepkowski, J. M., Powe, N. R., Laveist, T., Kuczmarski, M. F., and Zonderman, A. B. (2010). Healthy aging in neighborhoods of diversity across the life span (HANDLS): overcoming barriers to implementing a longitudinal, epidemiologic, urban study of health, race, and socioeconomic status. *Ethn. Dis.* 20, 267–275.

Eyles, D. W., Burne, T. H., and Mcgrath, J. J. (2013). Vitamin D, effects on brain development, adult brain function and the links between low levels of vitamin D and neuropsychiatric disease. *Front. Neuroendocrinol.* 34, 47–64. doi: 10.1016/j.yfrne.2012.07.001

Goodwill, A. M., Campbell, S., Simpson, S. Jr., Bisignano, M., Chiang, C., Dennerstein, L., et al. (2018). Vitamin D status is associated with executive function a decade later: data from the women's healthy ageing project. *Maturitas* 107, 56–62. doi: 10.1016/j.maturitas.2017.10.005

Greenlee, J. D., Oya, H., Kawasaki, H., Volkov, I. O., Severson, M. A. III, Howard, M. A. III, and Brugge, J. F. (2007). Functional connections within the human inferior frontal gyrus. *J. Comp. Neurol.* 503, 550–559. doi: 10.1002/cne.21405

Guo, Y. X., He, L. Y., Zhang, M., Wang, F., Liu, F., and Peng, W. X. (2016). 1,25-Dihydroxyvitamin D3 regulates expression of LRP1 and RAGE *in vitro* and *in vivo*, enhancing Abeta1-40 brain-to-blood efflux and peripheral uptake transport. *Neuroscience* 322, 28–38. doi: 10.1016/j.neuroscience.2016.01.041

Ispir, E., Serdar, M. A., Ozgurtas, T., Gulbahar, O., Akin, K. O., Yesildal, F., et al. (2015). Comparison of four automated serum vitamin B12 assays. *Clin. Chem. Lab. Med.* 53, 1205–1213. doi: 10.1515/cclm-2014-0843

Jacobs, H. I., Leritz, E. C., Williams, V. J., Van Boxtel, M. P., Van Der Elst, W., Jolles, J., et al. (2013). Association between white matter microstructure, executive functions, and processing speed in older adults: the impact of vascular health. *Hum. Brain Mapp.* 34, 77–95. doi: 10.1002/hbm.21412

Jenkinson, M., Bannister, P., Brady, M., and Smith, S. (2002). Improved optimization for the robust and accurate linear registration and motion correction of brain images. *Neuroimage* 17, 825–841. doi: 10.1006/nimg.2002.1132

Jenkinson, M., and Smith, S. (2001). A global optimisation method for robust affine registration of brain images. *Med. Image Anal.* 5, 143–156. doi: 10.1016/S1361-8415(01)00036-6

Jia, Z., Huang, X., Wu, Q., Zhang, T., Lui, S., Zhang, J., et al. (2010). High-field magnetic resonance imaging of suicidality in patients with major depressive disorder. *Am. J. Psychiatry* 167, 1381–1390. doi: 10.1176/appi.ajp.2010.09101513

Jones, D. K. (2008). Studying connections in the living human brain with diffusion MRI. *Cortex* 44, 936–952. doi: 10.1016/j.cortex.2008.05.002

Karakis, I., Pase, M. P., Beiser, A., Booth, S. L., Jacques, P. F., Rogers, G., et al. (2016). Association of serum vitamin D with the risk of incident dementia and subclinical indices of brain aging: the framingham heart study. *J. Alzheimers Dis.* 51, 451–461. doi: 10.3233/JAD-150991

Kruman, I.i, Culmsee, C., Chan, S. L., Kruman, Y., Guo, Z., Penix, L., and Mattson, M. P. (2000). Homocysteine elicits a DNA damage response in neurons that promotes apoptosis and hypersensitivity to excitotoxicity. *J. Neurosci.* 20, 6920–6926. doi: 10.1523/JNEUROSCI.20-18-06920.2000

Kuzma, E., Soni, M., Littlejohns, T. J., Ranson, J. M., Van Schoor, N. M., Deeg, D. J., et al. (2016). Vitamin D and memory decline: two population-based prospective studies. *J. Alzheimers. Dis.* 50, 1099–1108. doi: 10.3233/JAD-150811

Lee, C. C., Hsu, S. W., Huang, C. W., Chang, W. N., Chen, S. F., Wu, M. K., et al. (2017). Effects of homocysteine on white matter diffusion parameters in Alzheimer's disease. *BMC Neurol.* 17:192. doi: 10.1186/s12883-017-0970-7

Lee, Y. M., Ha, J. K., Park, J. M., Lee, B. D., Moon, E., Chung, Y. I., et al. (2016). Apolipoprotein E genotype modulates effects of vitamin B12 and homocysteine on grey matter volume in Alzheimer's disease. *Psychogeriatrics* 16, 3–11. doi: 10.1111/psyg.12109

Littlejohns, T. J., Kos, K., Henley, W. E., Lang, I. A., Annweiler, C., Beauchet, O., et al. (2016). Vitamin D and risk of neuroimaging abnormalities. *PLoS ONE* 11:e0154896. doi: 10.1371/journal.pone.0154896

McCaddon, A., and Miller, J. W. (2015). Assessing the association between homocysteine and cognition: reflections on Bradford Hill, meta-analyses, and causality. *Nutr. Rev.* 73, 723–735. doi: 10.1093/nutrit/nuv022

McCarrey, A. C., An, Y., Kitner-Triolo, M. H., Ferrucci, L., and Resnick, S. M. (2016). Sex differences in cognitive trajectories in clinically normal older adults. *Psychol. Aging* 31, 166–175. doi: 10.1037/pag0000070

McKay, N. S., Moreau, D., Henare, D. T., and Kirk, I. J. (2019). The brain-derived neurotrophic factor Val66Met genotype does not influence the grey or white matter structures underlying recognition memory. *Neuroimage* 197, 1–12. doi: 10.1016/j.neuroimage.2019.03.072

Melrose, R. J., Campa, O. M., Harwood, D. G., Osato, S., Mandelkern, M. A., and Sultzer, D. L. (2009). The neural correlates of naming and fluency deficits in Alzheimer's disease: an FDG-PET study. *Int. J. Geriatr. Psychiatry* 24, 885–893. doi: 10.1002/gps.2229

Michos, E. D., Carson, K. A., Schneider, A. L., Lutsey, P. L., Xing, L., Sharrett, A. R., et al. (2014). Vitamin D and subclinical cerebrovascular disease: the atherosclerosis risk in communities brain magnetic resonance imaging study. *JAMA Neurol.* 71, 863–871. doi: 10.1001/jamaneurol.2014.755

Miller, J. W. (2010). Vitamin D and cognitive function in older adults: are we concerned about vitamin D-mentia? *Neurology* 74, 13–15. doi: 10.1212/WNL.0b013e3181c719a2

Min, J. Y., and Min, K. B. (2016). The folate-vitamin B12 interaction, low hemoglobin, and the mortality risk from Alzheimer's disease. *J. Alzheimers Dis.* 52, 705–712. doi: 10.3233/JAD-151095

Moon, Y., Moon, W. J., Kwon, H., Lee, J. M., and Han, S. H. (2015). Vitamin D deficiency disrupts neuronal integrity in cognitively impaired patients. *J. Alzheimers Dis.* 45, 1089–1096. doi: 10.3233/JAD-143063

Moretti, R., Caruso, P., Dal Ben, M., Conti, C., Gazzin, S., and Tiribelli, C. (2017). Vitamin D, homocysteine, and folate in subcortical vascular dementia and Alzheimer dementia. *Front. Aging Neurosci.* 9:169. doi: 10.3389/fnagi.2017.00169

Owen, W. E., and Roberts, W. L. (2003). Comparison of five automated serum and whole blood folate assays. *Am. J. Clin. Pathol.* 120, 121–126. doi: 10.1309/L2U6HH5KAYG48L40

Pieters, B., Staals, J., Knottnerus, I., Rouhl, R., Menheere, P., Kessels, A., et al. (2009). Periventricular white matter lucencies relate to low vitamin B12 levels in patients with small vessel stroke. *Stroke* 40, 1623–1626. doi: 10.1161/STROKEAHA.108.523431

Powe, C. E., Evans, M. K., Wenger, J., Zonderman, A. B., Berg, A. H., Nalls, M., et al. (2013). Vitamin D-binding protein and vitamin D status of black Americans and white Americans. *N. Engl. J. Med.* 369, 1991–2000. doi: 10.1056/NEJMoa1306357

Prager, J. M., Thomas, C., Ankenbrandt, W. J., Meyer, J. R., Gao, Y., Ragin, A., et al. (2014). Association of white matter hyperintensities with low serum 25-hydroxyvitamin D levels. *AJNR Am. J. Neuroradiol.* 35, 1145-1149. doi: 10.3174/ajnr.A3840

R Foundation for Statistical Computing (2013). *R: A Language and Environment for Statistical Computing*. Vienna. Available online at: http://www.R-project.org/

Rankin, K. P., Gorno-Tempini, M. L., Allison, S. C., Stanley, C. M., Glenn, S., Weiner, M. W., et al. (2006). Structural anatomy of empathy in neurodegenerative disease. *Brain* 129, 2945–2956. doi: 10.1093/brain/awl254

Roher, A. E., Lowenson, J. D., Clarke, S., Woods, A. S., Cotter, R. J., Gowing, E., et al. (1993). beta-Amyloid-(1-42) is a major component of cerebrovascular amyloid deposits: implications for the pathology of Alzheimer disease. *Proc. Natl. Acad. Sci. U.S.A.* 90, 10836–10840. doi: 10.1073/pnas.90.22.10836

Rosenberg, I. H. (2008). Effects of folate and vitamin B12 on cognitive function in adults and the elderly. *Food Nutr. Bull.* 29, S132–S142. doi: 10.1177/15648265080292S118

Sachdev, P. S., Valenzuela, M., Wang, X. L., Looi, J. C., and Brodaty, H. (2002). Relationship between plasma homocysteine levels and brain atrophy in healthy elderly individuals. *Neurology* 58, 1539–1541. doi: 10.1212/WNL.58.10.1539

Schoenberg, M. R., and Scott, J. G. (2011). *The Little Black Book of Neuropsychology a Syndrome-Based Approach*. New York, NY; London: Springer.

Scott, T. M., Tucker, K. L., Bhadelia, A., Benjamin, B., Patz, S., Bhadelia, R., et al. (2004). Homocysteine and B vitamins relate to brain volume and white-matter changes in geriatric patients with psychiatric disorders. *Am. J. Geriatr. Psychiatry.* 12, 631–638. doi: 10.1097/00019442-200411000-00009

Selvin, S. (2004). *Statistical Analysis of Epidemiologic Data.* Oxford: Oxford University Press.

Shirafuji, N., Hamano, T., Yen, S. H., Kanaan, N. M., Yoshida, H., Hayashi, K., et al. (2018). Homocysteine increases tau phosphorylation, truncation and oligomerization. *Int. J. Mol. Sci.* 19:891. doi: 10.3390/ijms19030891

Smith, A. D., and Refsum, H. (2016). Homocysteine, B vitamins, and cognitive impairment. *Annu. Rev. Nutr.* 36, 211–239. doi: 10.1146/annurev-nutr-071715-050947

Snow, C. F. (1999). Laboratory diagnosis of vitamin B12 and folate deficiency: a guide for the primary care physician. *Arch. Intern. Med.* 159, 1289–1298. doi: 10.1001/archinte.159.12.1289

Stata (2019). *Statistics/Data Analysis: Release 16.0*. College Station, TX: Stata Corporation.

Tan, E. Y. L., Kohler, S., Hamel, R. E. G., Munoz-Sanchez, J. L., Verhey, F. R. J., and Ramakers, I. (2019). Depressive symptoms in mild cognitive impairment and the risk of dementia: a systematic review and comparative meta-analysis of clinical and community-based studies. *J. Alzheimers Dis.* 67, 1319–1329. doi: 10.3233/JAD-180513

Thacher, T. D., and Clarke, B. L. (2011). Vitamin D insufficiency. *Mayo Clin. Proc.* 86, 50–60. doi: 10.4065/mcp.2010.0567

Troesch, B., Weber, P., and Mohajeri, M. H. (2016). Potential links between impaired one-carbon metabolism due to polymorphisms, inadequate B-vitamin status, and the development of Alzheimer's disease. *Nutrients* 8:803. doi: 10.3390/nu8120803

US Department of Health & Human Services (2019). *The 2004 HHS Poverty Guidelines*. Available online at: https://aspe.hhs.gov/2004-hhs-poverty-guidelines (accessed September 2, 2019).

Vogiatzoglou, A., Refsum, H., Johnston, C., Smith, S. M., Bradley, K. M., De Jager, C., et al. (2008). Vitamin B12 status and rate of brain volume loss in community-dwelling elderly. *Neurology* 71, 826–832. doi: 10.1212/01.wnl.0000325581.26991.f2

Wakana, S., Jiang, H., Nagae-Poetscher, L. M., Van Zijl, P. C., and Mori, S. (2004). Fiber tract-based atlas of human white matter anatomy. *Radiology* 230, 77–87. doi: 10.1148/radiol.2301021640

Waldstein, S. R., Dore, G. A., Davatzikos, C., Katzel, L. I., Gullapalli, R., Seliger, S. L., et al. (2017). Differential associations of socioeconomic status with global brain volumes and white matter lesions in african american and white adults: the HANDLS SCAN study. *Psychosom. Med.* 79, 327–335. doi: 10.1097/PSY.0000000000000408

Weuve, J., Barnes, L. L., Mendes De Leon, C. F., Rajan, K. B., Beck, T., Aggarwal, N. T., et al. (2018). Cognitive aging in black and white Americans: cognition, cognitive decline, and incidence of Alzheimer disease dementia. *Epidemiology* 29, 151–159. doi: 10.1097/EDE.0000000000000747

World Health Organization (2015). "Serum and red blood cell folate concentrations for assessing folate status in populations," in *VMNIS|Vitamin and Mineral Nutrition Information System*, eds Department of Nutrition for Health and Development (NHD) (Geneva: World Health Organization), 1–7.

Wu, M. K., Lu, Y. T., Huang, C. W., Lin, P. H., Chen, N. C., Lui, C. C., et al. (2015). Clinical significance of cerebrovascular biomarkers and white matter tract integrity in Alzheimer disease: clinical correlations with neurobehavioral data in cross-sectional and after 18 months follow-ups. *Medicine (Baltimore)* 94:e1192. doi: 10.1097/MD.0000000000001192

Zou, K., Huang, X., Li, T., Gong, Q., Li, Z., Ou-Yang, L., et al. (2008). Alterations of white matter integrity in adults with major depressive disorder: a magnetic resonance imaging study. *J. Psychiatry Neurosci.* 33, 525–530.

Conflict of Interest: The authors declare that the research was conducted in the absence of any commercial or financial relationships that could be construed as a potential conflict of interest.

Vitamin D, folate and cobalamin status and change are related to brain volume and white matter integrity in urban adults

Beydoun et. al.

ONLINE SUPPLEMENTARY MATERIAL

Supplemental Method 1. Brain structural/diffusion (s) magnetic resonance imaging (MRI) and diffusion (d) MRI detailed description:

HANDLS description

sMRI

The T1-weighted MP-RAGE images covered the whole brain in a sagittal plane at a thickness of 1.2 mm for 160 slices (TR/TE/TI=2300/2.9/900 ms; FOV 25.6cm). These images were converted from sagittal to axial sections for comparative purposes.

The Section for Biomedical Image Analysis at the University of Pennsylvania developed in-house techniques to preprocess structural MRI scans. First, extra-cranial material on the T1-weighted images was removed using a multi-atlas registration method requiring minimal correction by hand (Doshi et al., 2013). Multiplicative intrinsic component optimization (MICO) method was used to correct for bias (Li et al., 2014). MUlti-atlas region Segmentation utilizing Ensembles (MUSE), segmented pre-processed images into a set of anatomical regions of interest (ROIs) (Doshi et al., 2016). MUSE integrates a broad ensemble of labeled templates by using a number of warping algorithms, regularization atlases and parameters (Doshi et al., 2016).

dMRI

Isotropic resolution images were acquired with an in-plane resolution of 2x2 mm and 2 mm slice thickness over a 22.4 cm FOV. A total of 66 slices at a TE = 122ms, TR = 3300ms, and flip angle = 90o were used. Eddy current effects were reduced by using bipolar diffusion. Diffusion weighting scheme was a 2-shell (b = 1000, 2500), optimized for uniform sampling of each shell and non-overlapping diffusion directions of 60 and 120 for each shell, respectively, and 6 b0 volumes. The image acquisition time was ten minutes.

Joint Linear Minimum Mean Squared Error denoising software (jLMMSE; Tristan-Vega and Aja-Fernandez, 2010) was used to de-noise the raw DWI data. The DT images were reconstructed by fitting the de-noised DWI data

using multivariate linear fitting. Motion correction was conducted with FSL' s "eddycorrect" tool (Andersson and Sotiropoulos, 2016).

Fractional Anisotropy (FA) – a widely established method for quantifying WMI sensitive to the degree of myelination, density, and organization of WM – was used to determine directionality of water diffusion in the brain. It measures the degree of anisotropy of the diffusion at the voxel level. It is derived from the variance of the average of the three eigenvalues of the diffusion tensor that are used to compute FA values, ranging from 0 to 1; 0 indicates completely unrestricted diffusion, and 1 denotes completely restricted diffusion. Computing the sum of the eigenvalues of the diffusion tensor yields the TR or mean diffusivity (MD), with a higher value indicative of poorer WMI. (Jones, 2008).

Quality assurance

The Core for Translational Research in Imaging @ Maryland (C-TRIM), managed by the Department of Diagnostic Radiology at UMB's School of Medicine, has instituted several quality control measures to ensure highest level of quality (and safety). The research dedicated scanner undergoes routine American College of Radiology mandated daily quality assurance(Mulkern et al., 2008). In addition, the AD Neuroimaging Initiative phantom is used to assess weekly signal-to-noise ratio and monthly structural distortions(Gunter et al., 2009). We periodically check the reliability of diffusion data by using the National Institutes of Standards and Technology diffusion phantom to ensure that the diffusion measurements from diffusion MRI are stable(phantom)

Supplemental Method 2: Additional covariates, LASSO regression and multiple imputations

A. Additional covariates:

A.1. Socio-demographic

Additional socio-demographic confounders included educational attainment (0≤High School (HS); 1=HS and 2≥HS), the Wide Range Achievement Test (WRAT) letter and word reading subtotal scores to measure literacy and marital status (1=married, 0=not married) (Beydoun et al., 2018).

A.2. Lifestyle

Smoking and drug use
Current use of opiate, marijuana or cocaine use ("current" *vs*. "never or former") and smoking status ("current" vs. "never or former") were considered.

Adiposity measures
Measured body mass index (BMI, kg/m^2), waist circumference and waist-hip-ratio were considered among potential confounders.

Healthy Eating Index 2010-
The Healthy Eating Index (HEI-2010) total score, based on two 24-hr recalls administered at baseline, was used as a measure of overall dietary quality. See steps for calculating HEI-2010 at http://appliedresearch.cancer.gov/tools/hei/tools.html and http://handls.nih.gov/06Coll-dataDoc.html.

Dietary Approaches to Stop Hypertension (DASH)

The score for DASH diet adherence, based on 8 nutrients, was determined for each participant using the formula reported by Mellen *et al*.(Mellen et al.). The nine target nutrients were total fat, saturated fat, protein, fiber, cholesterol, sodium, calcium, magnesium, and potassium. Micronutrient goals were expressed per 1000 kcal. The total DASH score was generated by the sum of all nutrient targets met. If the participant achieved the DASH target for a nutrient, a value of 1 was assigned, and if the intermediate target for a nutrient was achieved, a value of 0.5 was assigned. A value of zero was assigned if neither target was met. The maximum DASH score was 9; individuals meeting approximately half of the DASH targets (DASH score = 4.5) were considered DASH adherent (Mellen et al.).

Mean Adequacy Ratio (MAR)
Diet quality was also assessed using Nutrient Adequacy Ratio (NAR) and Mean Adequacy Ratio (MAR) scores(Murphy et al., 2006;Fanelli Kuczmarski et al., 2013). The NAR score was determined by taking each participant's daily intake of a nutrient divided by the Recommended Dietary Allowance (RDA) for that nutrient. NAR scores were determined for 17 micronutrients: vitamins A, C, D, E, B_6, B_{12}, folate, iron, thiamin, riboflavin, niacin, copper, zinc, calcium, magnesium, phosphorus, and selenium. The RDA was adjusted for participants' ages and sexes and vitamin C was adjusted for smokers(Murakami et al., 2019). The NAR score was converted into a percent with values exceeding 100 truncated to 100. MAR scores were calculated by averaging the NAR scores: MAR= (∑NAR scores)/17(Fanelli Kuczmarski et al., 2018). NAR and MAR were calculated separately for each daily-intake and then averaged. MAR scores, based on food intakes only, were used as the nutrient-based diet quality variable.

Supplemental use

The HANDLS dietary supplement questionnaire was adapted from the 2007 NHANES instrument.(Centers for Disease Control and Prevention, 2007) HANDLS participants provided supplement bottles during their dietary interview at the follow-up visit only (i.e. visit 2). Information on Over-The-Counter (OTC) vitamin and mineral supplements, antacids, prescription supplements, and botanicals were reported, and supplement users were asked about dose strength, dose amount consumed, length of supplement use (converted to days), frequency of use (daily, monthly, seasonally, annually), and if each supplement was taken the day prior to interview(Beydoun et al., 2018).

A HANDLS dietary supplement database was developed by trained nutritionists and registered dietitians. This database consisted of 4 files integrated to generate daily intake of each nutrient consumed by a dietary supplement user. [See detailed description at the HANDLS study website: https://handls.nih.gov/].

Depressive symptoms

Depressive symptoms were operationalized using the CES-D, at both baseline and follow-up. The 20-item CES-D is a self-reported symptom rating scale assessing affective and depressed mood.(Radloff, 1977) A score of ≥16 on the CES-D is reflective of elevated depressive symptoms (EDS), (Ramos et al., 2004) and predicts clinical depression based on the Diagnostic and Statistical Manual, fourth edition (DSM-IV) criteria.(Myers and Weissman, 1980) Four CES-D sub-domains exhibiting an invariant factor structure between The National Health and Nutrition Examination Survey I and pilot HANDLS data (Nguyen et al., 2004) were computed. We tested our hypotheses using total and domain-specific CES-D scores: **(1)** Somatic complaints; **(2)** Depressive affect; **(3)** Positive affect and **(4)** Interpersonal problems.(Nguyen et al., 2004)

A.3. Health-related

Baseline chronic conditions included self-reported history and biomarker-based measurement (as well as medication-based) of type 2 diabetes, hypertension, dyslipidemia, cardiovascular disease and inflammatory disease. Dyslipidemia was based on a combination of self-report, HDL, total cholesterol, triglyceride criteria as well as statin use. Similarly, type 2 diabetes was determined using a combination of self-report, serum glucose criteria and medication, as was the case for hypertension. In addition, a composite of cardiovascular disease history was added in which self-reported stroke, congestive heart failure, non-fatal myocardial infarction or atrial fibrillation were considered and combined into a yes/no variable. Similarly, inflammatory disease was a binary composite of multiple sclerosis, systemic lupus, gout, rheumatoid arthritis, psoriasis, Thyroid disorder and Crohn's disease. The use of NSAIDs (NSAIDs, prescription and over-the-counter) over the past two weeks as well as use of statins were considered separately as potential covariates.

A.4. Other biomarkers

All laboratory tests selected for this study were done at Quest Diagnostics, Chantilly, VA.

Serum cholesterol and atherogenic indices

Total cholesterol (TC), High density lipoprotein-cholesterol (HDL-C) and Triacylglycerols (TA) were assessed using a spectrophotometer (Olympus 5400). Low density lipoprotein-cholesterol (LDL-C) was calculated as TC-(HDL-C+TA/5) and directly measured in a sub-sample (N=236) also using a spectrophotometer (Olympus 5400). The correlation between those with baseline calculated LDL-C and those with measured LDL-C was r~0.95. From these measures, two relative measures were obtained, namely TC:HDL-C and LDL-C:HDL-C ratios. Those two relative measures, also termed "atherogenic indices" were previously studied in relation to various cardiovascular outcomes and were found to be positively associated with measures of atherosclerosis and coronary heart disease. (Nair et al., 2009;Manickam et al., 2011;Hisamatsu et al., 2014)

Serum uric acid (SUA)

SUA measurements are useful in the diagnosis and treatment of renal and metabolic disorders, including renal failure, gout, leukemia, psoriasis, starvation or other wasting conditions, and in patients receiving cytotoxic drugs. Using 1 ml of fasting blood serum, uric acid was measured using a standard spectrophotometry method. The reference range for adult men is 4.0-8.0 mg/dL, whereas for women, this range is cited as 2.5-7.0 mg/dL. (http://www.questdiagnostics.com/testcenter/TestDetail.action?ntc=905) Other reference ranges were also recently suggested and depend on the menopausal status of women. Those reference ranges are based on predictive value for

gout outcomes among healthy individuals and do not necessarily predict other pathologies. Thus, based on recent research evidence, a "normal" SUA value is suggested to be <6.0 mg/dL for all healthy adult individuals.

Serum albumin

Using 0.5-1 mL sample of plasma prepared with heparin and refrigerated for up to 30 days, albumin was measured with spectrophotometry, with an expected reference range of 3.6-5.1 g/dL(Beydoun et al., 2016b;Beydoun et al., 2019).

High sensitivity C-reactive protein (CRP)

High sensitivity CRP (hs-CRP) was analyzed with an immunoturbidimeter (Siemens/Behring Nephelometer II), using 0.5-1 mL of plasma, with the range 1-10 mg/dL indicating average or high cardiovascular risk and >10 mg/dL suggestive of an infection or a chronic inflammation.

Serum creatinine

Using participant fasting venous blood specimens, baseline serum creatinine was measured at the National Institute on Aging, Clinical Research Branch Core Laboratory, using a modified kinetic Jaffe method (CREA method, Dade Dimension X-Pand Clinical Chemistry System, Siemens Healthcare Diagnostics Inc., Newark, DE) for a small group of participants (n=88); while the majority of participants (n=1,528) had baseline serum creatinine analyzed at Quest Diagnostics, Inc. by isotope dilution mass spectrometry (IDMS) (Olympus America Inc., Melville, NY) and standardized to the reference laboratory, Cleveland Clinic. While inter-assay coefficients of variation (CV) for this sample could not be calculated due to the use of only one or the other measurement of creatinine at baseline, only intra-assay CVs (mean/SD) could be estimated and those were 0.192 and 0.187 for the CREA and the IDMS methods, respectively.

HbA1c

Glycated hemoglobin is derived from the nonenzymatic addition of glucose to amino groups of hemoglobin. HbA1c is a specific glycated hemoglobin that results from the attachment of glucose to the N-terminal valine of the hemoglobin b-chain. Numerous assays were subsequently developed to measure glycated hemoglobins. The principle of all methods is to separate the glycated and nonglycated forms of hemoglobin(Beydoun et al., 2016a). This can be accomplished based on differences in charge (usually by HPLC) or structure (usually immunoassays or boronate affinity chromatography). In this study, the method adopted was HPLC (Quest diagnostics).

White blood cell inflammatory markers

Fasting blood samples were collected from participants at baseline and follow-up to determine total white blood cell count, (K/mm^3), using electronic Cell Sizing, counting, cytometry and microscopy. (http://www.questdiagnostics.com/testcenter/TestDetail.action?ntc=7064).

Red cell distribution width (RDW), hemoglobin and other iron status measures

RDW

RDW was measured by automated Coulter DXH 800 hematology analyzer as part of peripheral complete blood count (Beckman Coulter, Brea, CA), and was expressed as coefficient of variation (%) of red blood cell volume distribution. Regular calibration was performed every 3 months on the hematology analyzer and quality control was performed according to the manufacturer's recommendations.(Diagnostics) There are usually two RDW measurements used for clinical purposes, namely the RDW-coefficient of variation (CV, unit: %), which we used in this study, and the RDW-Standard Deviation (SD, unit: fL) from which RDW-CV is derived. In fact, RDW-CV=RDW-SD×100/MCV, where MCV is the mean cell volume. The normal range for RDW-CV is 11.0 - 15.0%. Thus, the RDW-CV (%) depends on both the width of the distribution (normal range: 40-55 fL) curve and the MCV.(techs, 2019)

Hemoglobin (Hb)

Similarly, using electronic cell sizing/cytometry/microscopy, Hb was assayed from a sample of 1 ml of blood drawn from participants after overnight fast, and refrigerated up to 6 days (Quest diagnostics).

Other iron status markers

Ferritin: Ferritin is decreased in iron deficiency anemia and increase in iron overload. It is measured with immunoassay with reference ranges of 20-380 ng/mL among men and 10-232 ng/mL among women.(Diagnostics)

Erythrocyte Sedimentation Rate (ESR): Using 5 mL of refrigerated whole blood stored in lavender-top EDTA tubes, the ESR was tested within 24 hr of blood draw. This test used automated modified Westergren photochemical capillary stopped flow kinetic analysis.(Diagnostics;Larsson and Hansson, 2004) The Mayo clinic reports a reference of 0-22 mm/hr for men and 0-29 mm/hr for women(Mayo Clinic, 2017) and is considered a proxy measure for serum fibrinogen.(Yin et al., 2017)

Serum iron: 0.5-1 mL of fasting serum was collected, transported at room temperature (with heparin added) and refrigerated or frozen subsequently. Serum iron was measured with spectrophotometry, (Diagnostics;Samarina and Proskurnin, 2015) with reference ranges for men aged ≥30y set at 50-180 µg/dL and for women: 20-49y (40-190 µg /dL) and 50+y(45-160 µg /dL). (Diagnostics)

MCV: Also known as erythrocyte mean corpuscular volume, MCV is measured using standard electronic cell sizing/counting/cytometry/microscopy. Similar to other hemogram measures (e.g. ESR), a microtainer 1 mL whole blood in an EDTA (lavender-top) tube was transported at room temperature to the laboratory facility.(Diagnostics)

MCH: The hematologic index MCH was calculated as follows: MCH = Hb/RBC.

B. Least absolute shrinkage and selection operator (LASSO) regression procedure

In order to select the appropriate set of predictive model for each of the 3 vitamins, we used statistical learning method for variable selection known as adaptive LASSO, and compared it to cross-validation LASSO (cvLASSO) and lowest BIC LASSO. Socio-demographic variables, namely age, sex, race/ethnicity, poverty status were force entered in all models as fixed terms. The LASSO then selected among the other covariates listed above, the ones that should be retained. Covariates were imputed using chained equations (5 imputations, 10 iterations), accounting for their level of measurement. Socio-demographic factors were entered into all the chained equations. Continuous covariates were entered as outcomes in a series of linear regression models, while binary and categorical variables were entered into a series of multinomial logit regression models.

LASSO is a covariate selection methodology that is superior to both generalized linear models without covariate selection and the usually applied stepwise or backward elimination process.(Zou, 2006) In fact, stepwise selection is often trapped into a local optimal solution rather than the global optimal solution and backward elimination can be time-consuming given the large number of variables in the full model.(Zou, 2006) These methods often ignore stochastic errors or uncertainty incurred during variable selection, with the LASSO estimate being defined as follows:

$$\beta(\text{lasso}) = \arg min_{\beta} || \, y - \sum_{j=1}^{p} x_j \beta_j \, ||^2 + \lambda \sum_{j=1}^{p} |\beta_j \, |$$

with λ being a nonnegative regularization parameter.(Zou, 2006) The second term of the equation termed the "l1 penalty" is a key portion of this equation ensuring the success of the lasso method of covariate selection. In fact, this method was shown to discover the right sparse representation of the model, given certain conditions. Nevertheless, this method can produce biased estimates for larger coefficients. Thus, there a number of scenarios whereby the LASSO can yield inconsistent results. More recently, several related methods have been developed and validated against each other. It was shown that an adaptive version of the LASSO gave more consistent findings, particularly when compared with another popular variable selection technique known as the nonnegative garotte.

In our modeling approach, we used this convex optimization technique with l_1 constraint known as adaptive LASSO as one of three methods to select the final linear regression models. The model is trained on a random half sample of the total population (first imputation out of 5) and validated against the other half sample to check robustness of findings, by comparing R^2 between samples. One model was selected among the cvLASSO, adaptive LASSO or minBIC LASSO, depending on how close the R^2 are between half-samples. This parsimonious model selected for each of 3 vitamins (measured at v_1) as 6 potential outcomes is then run on the entire population and a backward elimination process is carried out to keep only significant covariates at type I error of 0.10. Thus, the selected model through LASSO was used as a starting point for further backward elimination. Backward elimination was conducted on the imputed data for the entire sample, rather than the half sample for the first imputation.

In our analysis, the following LASSO models were selected and the final model included is shown also in this Table.

	Selected covariates[1]			
	cvLASSO	**Min BIC LASSO**	**Adaptive LASSO**	**Reduced model**
Vitamin D (v1)	Sex, race, pir, age, B12, Folate, BMI, Cholesterol, ESR, MCV, Iron, Triglycerides, MAR, Albumin, education, Uric acid, MCH, NSAIDs, statins, Diabetes, WBC, CVD, HDL, RDW, education, current drug use, creatinine, DASH, Ferritin	**Sex, race, pir, age B12, Folate, BMI, Cholesterol, MCV, MAR, Albumin**	Sex, race, pir, age, B12, Folate, BMI, Cholesterol, ESR, MCV, Iron, Triglycerides, MAR, Albumin, education, Uric acid, NSAIDs, statins, Diabetes, WBC, CVD	**Sex, race, pir, age, B12, Folate, BMI, MCV, Albumin**
Folate (v1)	Age, sex, pir, race, B12, Vitamin D, MAR, Ferritin, iron, smoking, MCH, education, DASH, diagnosed diabetes, Albumin, CES-D, diagnosed hypertension, cholesterol, CRP, Hemoglobin, HbA1c, diagnosed dyslipidemia, RDW, NSAIDs, married.	**Age, sex, pir, race, B12, Vitamin D, MAR, Ferritin, iron, smoking, MCH, education, DASH, Diabetes, Albumin, CES-D, hypertension, cholesterol, CRP, Hemoglobin, HbA1c, diagnosed dyslipidemia, RDW, NSAIDs, married.**	Age, sex, pir, race, B12, Vitamin D, MAR, Ferritin, iron, smoking, MCH, education, DASH, Diabetes, Albumin, CES-D, hypertension, cholesterol, CRP, Hemoglobin, HbA1c, diagnosed dyslipidemia, RDW, NSAIDs.	**Age, sex, pir, race, B12, Vitamin D, MAR, Ferritin, iron, smoking, DASH, Albumin, Hemoglobin, RDW**
B-12 (v1)	Age, sex, race, pir, vitamin D, Folate, vitamin supplement	**Age, sex, race, pir, vitamin D, Folate, vitamin**	Age, sex, race, pir, vitamin D, Folate, vitamin supplement use,	**Age, sex, race, pir, vitamin D, Folate,**

	use, HEI-2010, Ferritin, RDW, ESR, Triglycerides, MCH, Cholesterol, married albumin.	**supplement use, HEI-2010, RDW.**	HEI-2010, Ferritin, RDW, ESR, Triglycerides, MCH, Cholesterol.	**vitamin supplement use, HEI-2010, RDW.**

Abbreviations: B-12=vitamin B-12 (cobalamin); BIC=Bayesian information criterion; BMI=Body Mass Index; CES-D=Center for Epidemiologic Studies-Depression; CRP=C-reactive Protein; cv=cross-validation; CVD=Self-reported cardiovascular disease; DASH=Dietary Approaches to Stop Hypertension; ESR=Erythrocyte Sedimentation Rate; HbA1c=Glycated hemoglobin; HDL=High Density Lipoprotein Cholesterol; LASSO= Least absolute shrinkage and selection operator; HEI-2010=Healthy Eating Index, 2010 revision; MAR=Mean Adequacy Ratio; MCH=Mean cell hemoglobin; MCV=Mean Cell Volume; NSAIDS=Non-Steroidal Anti-inflammatory Drugs; RDW=Red cell distribution Width; WBC=White Blood Cells; WHR=Waist-Hip-Ratio

[1]Bolded sets of covariates are the ones that are selected at each step of the model selection process. A full row of bolded sets of covariates indicates that the selection process is equivalent and that backward elimination did not reduce the model further.

Supplemental Table 1: BRAIN ATLAS NOMENCLATURE FOR sMRI data[1,2,3]

ROI_INDEX	NUM_VOX	TISSUE_SEG	HEMISPHERE	SUBGROUP_0	SUBGROUP_1	SUBGROUP_2	ROI_NAME
95	12872	WM	B	CC			corpus callosum
71	4899.8	GM	B	CEREBELLUM			Cerebellar Vermal Lobules I-V
73	2858.8	GM	B				Cerebellar Vermal Lobules VIII-X
72	2266.9	GM	B				Cerebellar Vermal Lobules VI-VII
39	54583	GM	L				Left Cerebellum Exterior
41	15501	WM	L				Left Cerebellum White Matter
38	54379	GM	R				Right Cerebellum Exterior
40	15459	WM	R				Right Cerebellum White Matter
30	585.9	GM	L	DEEP_WM_GM	BASAL_GANGLIA		Left Accumbens Area
37	3578.9	GM	L				Left Caudate
56	1597.6	GM	L				Left Pallidum
58	4942.3	GM	L				Left Putamen
23	526	GM	R				Right Accumbens Area
36	3651.5	GM	R				Right Caudate
55	1638.8	GM	R				Right Pallidum
57	4726	GM	R				Right Putamen
60	8574.1	GM	L		DEEP_GM		Left Thalamus Proper
59	8256.3	GM	R				Right Thalamus Proper
92	2887.7	WM	L		DEEP_WM		anterior limb of internal capsule left
91	3393.3	WM	R				anterior limb of internal capsule right
90	673.6	WM	L				fornix left
89	517.5	WM	R				fornix right
94	2416.3	WM	L				posterior limb of internal

							capsule inc. cerebral peduncle left
93	2480.5	WM	R				posterior limb of internal capsule inc. cerebral peduncle right
32	993.7	GM	L				Left Amygdala
75	586.5	GM	L				Left Basal Forebrain
48	3597.7	GM	L				Left Hippocampus
31	1021.3	GM	R				Right Amygdala
76	593.1	GM	R				Right Basal Forebrain
47	3704.7	GM	R				Right Hippocampus
105	1897.7	GM	L	FRONTAL	FRONTAL_GM	FRONTAL_INFERIOR_GM	Left AOrG anterior orbital gyrus
137	3015.9	GM	L				Left LOrG lateral orbital gyrus
147	4637.3	GM	L				Left MOrG medial orbital gyrus
179	2915.7	GM	L				Left POrG posterior orbital gyrus
104	2244.9	GM	R				Right AOrG anterior orbital gyrus
136	2864.1	GM	R				Right LOrG lateral orbital gyrus
146	4526.7	GM					Right MOrG medial orbital gyrus
178	2504.8	GM	R				Right POrG posterior orbital gyrus
103	4749.1	GM	L			FRONTAL_INSULAR_GM	Left AIns anterior insula
173	2479.5	GM	L				Left PIns posterior insula
102	4600.1	GM	R				Right AIns anterior insula
172	2532	GM	R				Right PIns posterior insula
121	4392.8	GM	L			FRONTAL_LATERAL_GM	Left FRP frontal pole
143	22847	GM	L				Left MFG middle frontal gyrus
163	3747	GM	L				Left OpIFG opercular part of the

							inferior frontal gyrus
165	1901.2	GM	L				Left OrIFG orbital part of the inferior frontal gyrus
183	14665	GM	L				Left PrG precentral gyrus
191	16867	GM	L				Left SFG superior frontal gyrus
205	5256.2	GM	L				Left TrIFG triangular part of the inferior frontal gyrus
120	4673.7	GM	R				Right FRP frontal pole
142	22580	GM	R				Right MFG middle frontal gyrus
162	4094.1	GM	R				Right OpIFG opercular part of the inferior frontal gyrus
164	1944.4	GM	R				Right OrIFG orbital part of the inferior frontal gyrus
182	14641	GM	R				Right PrG precentral gyrus
190	16697	GM	R				Right SFG superior frontal gyrus
204	4522.4	GM	R				Right TrIFG triangular part of the inferior frontal gyrus
125	2920.3	GM	L			FRONTAL_MEDIAL_GM	Left GRe gyrus rectus
141	2245.2	GM	L				Left MFC medial frontal cortex
151	3081.3	GM	L				Left MPrG precentral gyrus medial segment
153	8737	GM	L				Left MSFG superior frontal gyrus medial segment
187	1220.8	GM	L				Left SCA subcallosal area
193	6723.3	GM	L				Left SMC supplementary motor cortex

124	2699.9	GM	R				Right GRe gyrus rectus
140	2202.6	GM	R				Right MFC medial frontal cortex
150	2944.5	GM	R				Right MPrG precentral gyrus medial segment
152	9415.8	GM	R				Right MSFG superior frontal gyrus medial segment
186	1236	GM	R				Right SCA subcallosal area
192	6368.8	GM	R				Right SMC supplementary motor cortex
113	4466.1	GM	L			FRONTAL_OPERCULAR_GM	Left CO central operculum
119	2489.9	GM	L				Left FO frontal operculum
175	2768.9	GM	L				Left PO parietal operculum
112	4691.3	GM	R				Right CO central operculum
118	2548.3	GM	R				Right FO frontal operculum
174	2414.5	GM	R				Right PO parietal operculum
82	91872	WM	L		FRONTAL_WM		frontal lobe WM left
81	95088	WM	R				frontal lobe WM right
101	5262.2	GM	L	LIMBIC	LIMBIC_GM	LIMBIC_CINGULATE_GM	Left ACgG anterior cingulate gyrus
139	5335.1	GM	L				Left MCgG middle cingulate gyrus
167	5181.6	GM	L				Left PCgG posterior cingulate gyrus
100	4782.3	GM	R				Right ACgG anterior cingulate gyrus
138	5475.1	GM	R				Right MCgG middle cingulate gyrus
166	4324.3	GM	R				Right PCgG posterior cingulate gyrus

117	1887.4	GM	L			LIMBIC_MEDIALTEMPORAL_GM	Left Ent entorhinal area
171	3536.5	GM	L				Left PHG parahippocampal gyrus
116	2120.6	GM	R				Right Ent entorhinal area
170	3257.5	GM	R				Right PHG parahippocampal gyrus
161	5087.5	GM	L	OCCIPITAL	OCCIPITAL_GM	OCCIPITAL_INFERIOR_GM	Left OFuG occipital fusiform gyrus
160	4857.3	GM	R				Right OFuG occipital fusiform gyrus
129	7403.4	GM	L			OCCIPITAL_LATERAL_GM	Left IOG inferior occipital gyrus
145	7232.9	GM	L				Left MOG middle occipital gyrus
157	4297.6	GM	L				Left OCP occipital pole
197	4152	GM	L				Left SOG superior occipital gyrus
128	7633	GM	R				Right IOG inferior occipital gyrus
144	6792.1	GM	R				Right MOG middle occipital gyrus
156	4054.5	GM	R				Right OCP occipital pole
196	4967	GM	R				Right SOG superior occipital gyrus
109	3635.5	GM	L			OCCIPITAL_MEDIAL_GM	Left Calc calcarine cortex
115	5314.7	GM	L				Left Cun cuneus
135	8386.3	GM	L				Left LiG lingual gyrus
108	3543.7	GM	R				Right Calc calcarine cortex
114	5884.9	GM	R				Right Cun cuneus
134	8366	GM	R				Right LiG lingual gyrus
84	22742	WM	L		OCCIPITAL_WM		occipital lobe WM left

83	22799	WM	R				occipital lobe WM right
107	9939.4	GM	L	PARIETAL	PARIETAL_GM	PARIETAL_LATERAL_GM	Left AnG angular gyrus
177	13594	GM	L				Left PoG postcentral gyrus
195	9984.3	GM	L				Left SMG supramarginal gyrus
199	11733	GM	L				Left SPL superior parietal lobule
106	11564	GM	R				Right AnG angular gyrus
176	11681	GM	R				Right PoG postcentral gyrus
194	9193	GM	R				Right SMG supramarginal gyrus
198	11792	GM	R				Right SPL superior parietal lobule
149	1400.3	GM	L			PARIETAL_MEDIAL_GM	Left MPoG postcentral gyrus medial segment
169	11737	GM	L				Left PCu precuneus
148	1162.5	GM	R				Right MPoG postcentral gyrus medial segment
168	11732	GM	R				Right PCu precuneus
86	47237	WM	L		PARIETAL_WM		parietal lobe WM left
85	44217	WM	R				parietal lobe WM right
123	8077.2	GM	L	TEMPORAL	TEMPORAL_GM	TEMPORAL_INFERIOR_GM	Left FuG fusiform gyrus
122	8000.9	GM	R				Right FuG fusiform gyrus
133	12612	GM	L			TEMPORAL_LATERAL_GM	Left ITG inferior temporal gyrus
155	15794	GM	L				Left MTG middle temporal gyrus
201	8451.3	GM	L				Left STG superior temporal gyrus
203	8632.1	GM	L				Left TMP temporal pole
132	12693	GM	R				Right ITG inferior

							temporal gyrus
154	16085	GM	R				Right MTG middle temporal gyrus
200	9031.2	GM	R				Right STG superior temporal gyrus
202	8883.7	GM	R				Right TMP temporal pole
181	2629.8	GM	L			TEMPORAL_SUPRATEMPORAL_GM	Left PP planum polare
185	2511.3	GM	L				Left PT planum temporale
207	1821.1	GM	L				Left TTG transverse temporal gyrus
180	2448.5	GM	R				Right PP planum polare
184	2325.5	GM	R				Right PT planum temporale
206	1529.1	GM	R				Right TTG transverse temporal gyrus
88	54535	WM	L		TEMPORAL_WM		temporal lobe WM left
87	55391	WM	R				temporal lobe WM right
4	636.8	VN	B	VENTRICLE			3rd Ventricle
11	1959.6	VN	B				4th Ventricle
50	304.9	VN	L				Left Inf Lat Vent
52	7954.9	VN	L				Left Lateral Ventricle
49	352.9	VN	R				Right Inf Lat Vent
51	6629.5	VN	R				Right Lateral Ventricle
35	18492	NONE	B				Brain Stem
46	1011.6	CSF	B				CSF
62	5192.8	NONE	L				Left Ventral DC
64	36.5	NONE	L				Left vessel
61	4998.9	NONE	R				Right Ventral DC
63	33.3	NONE	R				Right vessel

[1]Shaded in light orange: Analysis A which consisted of TOTALBRAIN, WM and GM as alternative outcomes.

[2]Shaded in light green: Analysis B which consisted of GM//WM categorized by larger regions: OCCIPITAL, PARIETAL, TEMPORAL and FRONTAL. This analysis included R and L summed together for each large region.

[3]Shaded in light gray: Analysis C which consisted of all available smaller regions. Excluded regions due to missing data are the ones in the last column that are not highlighted in gray. Additional regions included: Optic chiasm, Lesion Volume.

Supplemental Table 2: Regions of Interest (ROI) used for dMRI measures: Fractional anisotropy (FA) and trace (TR)[1]

LEFT BRAIN			
1	SPG_L	Superior Parietal Gyrus Left	GM
2	CingG_L	Cingulate Gyrus Left	GM
3	SFG_L	Superior Frontal Gyrus Left	GM
4	MFG_L	Middle Frontal Gyrus Left	GM
5	IFG_L	Inferior Frontal Gyrus Left	GM
6	PrCG_L	Precentral Gyrus Left	GM
7	PoCG_L	Postcentral Gyrus Left	GM
8	AG_L	Angular Gyrus Left	GM
9	PrCu_L	Pre-Cuneus Left	GM
10	Cu_L	Cuneus Left	GM
11	LG_L	Lingual Gyrus Left	GM
12	Fu_L	Fusiform Gyrus Left	GM
13	PHG_L	Parahippocampal Gyrus Left	GM
14	SOG_L	Superior Occipital Gyrus Left	GM
15	IOG_L	Inferior Occipital Gyrus	GM
16	MOG_L	Middle Occipital Gyrus	GM
17	ENT_L	Entorhinal Area	GM
18	STG_L	Superior Temporal Gyrus	GM
19	ITG_L	Inferior Temporal Gyrus	GM
20	MTG_L	Middle Temporal Gyrus	GM
21	LFOG_L	Lateral Fronto-Orbital Gyrus	GM
22	MFOG_L	Middle Fronto-Orbital Gyrus	GM
23	SMG_L	Supramarginal Gyrus	GM
24	RG_L	Gyrus Rectus	GM
25	Ins_L	Insular	GM
26	Amyg_L	Amygdala	GM
27	Hippo_L	Hippocampus	GM
28	Cerebrellum_L	Cerebellum	GM
29	CST_L	Corticospinal Tract Left	WM
30	ICP_L	Inferior Cerebellar Peduncle Left	WM
31	ML_L	Medial Lemniscus Left	WM/GM
32	SCP_L	Superior Cerebellar Peduncle Left	WM
33	CP_L	Cerebellar Peduncle Left	WM
34	ALIC_L	Anterior Limb of Internal Capsule Left	WM
35	PLIC_L	Posterior Limb of Internal Capsule Left	WM
36	PTR_L	Posterior Thalamic Radiation (Include Optic Radiation) Left	WM

37	ACR_L	Anterior Corona Radiata Left	WM
38	SCR_L	Superior Corona Radiata Left	WM
39	PCR_L	Posterior Corona Radiata Left	WM
40	CGC_L	Cingulum (Cingulate Gyrus) Left	WM
41	CGH_L	Cingulum (Hippocampus) Left	WM
42	Fx/ST_L	Fornix (Cres) / Stria Terminalis (Can Not Be Resolved With Current Resolution) Left	WM
43	SLF_L	Superior Longitudinal Fasciculus Left	WM
44	SFO_L	Superior Fronto-Occipital Fasciculus (Could Be A Part of Anterior Internal Capsule) Left	WM
45	IFO_L	Inferior Fronto-Occipital Fasciculus Left	WM
46	SS_L	Sagittal Stratum (Include Inferior Longitidinal Fasciculus And Inferior Fronto-Occipital Fasciculus) Left	WM
47	EC_L	External Capsule Left	WM
48	UNC_L	Uncinate Fasciculus Left	WM
49	PCT_L	Pontine Crossing Tract (A Part of Mcp) Left	WM
50	MCP_L	Middle Cerebellar Peduncle Left	WM
51	FX_L	Fornix (Column And Body of Fornix) Left	WM
52	GCC_L	Genu of Corpus Callosum Left	WM
53	BCC_L	Body of Corpus Callosum Left	WM
54	SCC_L	Splenium of Corpus Callosum Left	WM
55	RLIC_L	Retrolenticular Part of Internal Capsule Left	WM
56	REDNC_L	Red Nucleus Left	GM
57	SNIGRA_L	Substancia Nigra Left	GM
58	TAP_L	Tapatum Left	GM
59	Caud_L	Caudate Nucleus Left	GM
60	Put_L	Putamen Left	GM
61	Thal_L	Thalamus Left	GM
62	GP_L	Globus Pallidus Left	GM
63	Midbrain_L	Midbrain Left	GM
64	Pons_L	Pons Left	WM
65	Medulla_L	Medulla Left	WM/GM
66	SPWM_L	Superior Parietal WM Left	WM
67	Cingwm	Cingulum WM Left	WM
68	SFWM_L	Superior Frontal WM Left	WM
69	MFWM_L	Middle Frontal WM Left	WM
70	IFWM_L	Inferior Frontal WM Left	WM
71	PrCWM_L	Precentral WM Left	WM
72	PoCWM_L	Postcentral WM Left	WM
73	AWM_L	Angular WM Left	WM
74	PrCuWM_L	Pre-Cuneus WM Left	WM
75	CuWM_L	Cuneus WM Left	WM

76	LWM_L	Lingual WM Left	WM
77	Fu_WM_L	Fusiform WM Left	WM
78	SOWM_L	Superior Occipital WM Left	WM
79	IOWM_L	Inferior Occipital WM Left	WM
80	MOWM_L	Middle Occipital WM Left	WM
81	STwm_L	Superior Temporal WM Left	WM
82	ITWM_L	Inferior Temporal WM Left	WM
83	MTWM_L	Middle Temporal WM Left	WM
84	LFOWM_L	Lateral Fronto-Orbital WM Left	WM
85	MFOWM_L	Middle Fronto-Orbital WM Left	WM
86	SMWM_L	Supramarginal WM Left	WM
87	RGWM_L	Rectus WM Left	WM
88	Cerebrellumwm_L	Cerebellum WM Left	WM
RIGHT BRAIN			
89	SPG_R	Superior Parietal Gyrus Right	GM
90	CingG_R	Cingulate Gyrus Right	GM
91	SFG_R	Superior Frontal Gyrus Right	GM
92	MFG_R	Middle Frontal Gyrus Right	GM
93	IFG_R	Inferior Frontal Gyrus Right	GM
94	PrCG_R	Precentral Gyrus Right	GM
95	PoCG_R	Postcentral Gyrus Right	GM
96	AG_R	Angular Gyrus Right	GM
97	PrCu_R	Pre-Cuneus Right	GM
98	Cu_R	Cuneus Right	GM
99	LG_R	Lingual Gyrus Right	GM
100	FuG_R	Fusiform Gyrus Right	GM
101	PHG_R	Parahippocampal Gyrus Right	GM
102	SOG_R	Superior Occipital Gyrus Right	GM
103	IOG_R	Inferior Occipital Gyrus Right	GM
104	MOG_R	Middle Occipital Gyrus Right	GM
105	ENT_R	Entorhinal Area Right	GM
106	STG_R	Superior Temporal Gyrus Right	GM
107	ITG_R	Inferior Temporal Gyrus Right	GM
108	MTG_R	Middle Temporal Gyrus Right	GM
109	LFOG_R	Lateral Fronto-Orbital Gyrus Right	GM
110	MFOG_R	Middle Fronto-Orbital Gyrus Right	GM
111	SMG_R	Supramarginal Gyrus Right	GM
112	RG_R	Gyrus Rectus Right	GM
113	Ins_R	Insular Right	GM
114	Amyg_R	Amygdala Right	GM
115	Hippo_R	Hippocampus Right	GM

116	Cerebellum_R	Cerebellum Right	GM
117	CST_R	Corticospinal Tract Right	WM
118	ICP_R	Inferior Cerebellar Peduncle Right	WM
119	ML_R	Medial Lemniscus Right	WM/GM
120	SCP_R	Superior Cerebellar Peduncle Right	WM
121	CP_R	Cerebellar peduncle, Right	
122	ALIC_R	Anterior Limb of Internal Capsule Right	WM
123	PLIC_R	Posterior Limb of Internal Capsule Right	WM
124	PTR_R	Posterior Thalamic Radiation (Include Optic Radiation) Right	WM
125	ACR_R	Anterior Corona Radiata Right	WM
126	SCR_R	Superior Corona Radiata Right	WM
127	PCR_R	Posterior Corona Radiata Right	WM
128	CGC_R	Cingulum (Cingulate Gyrus) Right	WM
129	CGH_R	Cingulum (Hippocampus) Right	WM
130	Fx/ST_R	Fornix (Cres) / Stria Terminalis (Can Not Be Resolved With Current Resolution) Right	WM
131	SLF_R	Superior Longitudinal Fasciculus Right	WM
132	SFO_R	Superior Fronto-Occipital Fasciculus (Could Be A Part of Anterior Internal Capsule) Right	WM
133	IFO_R	Inferior Fronto-Occipital Fasciculus Right	WM
134	SS_R	Sagittal Stratum (Include Inferior Longitidinal Fasciculus And Inferior Fronto-Occipital Fasciculus) Right	WM
135	EC_R	External Capsule Right	WM
136	UNC_R	Uncinate Fasciculus Right	WM
137	PCT_R	Pontine Crossing Tract (A Part of MCP) Right	WM
138	MCP_R	Middle Cerebellar Peduncle Right	WM
139	FX_R	Fornix (Column And Body of Fornix) Right	WM
140	GCC_R	Genu of Corpus Callosum Right	WM
141	BCC_R	Body of Corpus Callosum Right	WM
142	SCC_R	Splenium of Corpus Callosum Right	WM
143	RLIC_R	Retrolenticular Part of Internal Capsule Right	WM
144	REDNC_R	Red Nucleus Right	GM
145	SNIGRA_R	Substancia Nigra Right	GM
146	TAP_R	Tapatum Right	GM
147	Caud_R	Caudate Nucleus Right	GM
148	Put_R	Putamen Right	GM
149	Thal_R	Thalamus Right	GM
150	GP_R	Globus Pallidus Right	GM
151	Midbrain_R	Midbrain Right	GM
152	Pons_R	Pons Right	WM
153	Medulla_R	Medulla Right	WM/GM
154	SPwm_R	Superior Parietal WM Right	WM
155	Cingwm_R	Cingulum WM Right	WM

156	**SFWM_R**	**Superior Frontal WM Right**	**WM**
157	**MFWM_R**	**Middle Frontal WM Right**	**WM**
158	**IFWM_R**	**Inferior Frontal WM Right**	**WM**
159	**PrCWM_R**	**Precentral WM Right**	**WM**
160	**PoCWM_R**	**Postcentral WM Right**	**WM**
161	**AWM_R**	**Angular WM Right**	**WM**
162	**PrCuWM_R**	**Pre-Cuneus WM Right**	**WM**
163	**CuWM_R**	**Cuneus WM Right**	**WM**
164	**LWM_R**	**Lingual WM Right**	**WM**
165	**Fuwm_R**	**Fusiform WM Right**	**WM**
166	**SOWM_R**	**Superior Occipital WM Right**	**WM**
167	**IOWM_R**	**Inferior Occipital WM Right**	**WM**
168	**MOWM_R**	**Middle Occipital WM Right**	**WM**
169	**STWM_R**	**Superior Temporal WM Right**	**WM**
170	**ITWM_R**	**Inferior Temporal WM Right**	**WM**
171	**MTWM_R**	**Middle Temporal WM Right**	**WM**
172	**LFOWM_R**	**Lateral Fronto-Orbital WM Right**	**WM**
173	**MFOWM_R**	**Middle Fronto-Orbital WM Right**	**WM**
174	**SMWM_R**	**Supramarginal WM Right**	**WM**
175	**RGWM_R**	**Rectus WM Right**	**WM**
176	**Cerebrellumwm_R**	**Cerebellum WM Right**	**WM**

[1]Right and Left measures of FA and TR were averaged out before analyses C and D was carried out. This resulted in 98 measures in total, 49 for FA and 49 for TR, when excluding measures with missing data. Measures included in the analysis are bolded and in red font. All others are excluded. In addition, cerebellum wm TR (Right and Left) were only available for 85 subjects, as was the case for SNIGRA FA/TR (Right and Left). TR is also known as mean diffusivity or MD.

Supplemental References:

Andersson, J.L.R., and Sotiropoulos, S.N. (2016). An integrated approach to correction for off-resonance effects and subject movement in diffusion MR imaging. *Neuroimage* 125**,** 1063-1078.

Beydoun, M.A., Beydoun, H.A., Mode, N., Dore, G.A., Canas, J.A., Eid, S.M., and Zonderman, A.B. (2016a). Racial disparities in adult all-cause and cause-specific mortality among us adults: mediating and moderating factors. *BMC Public Health* 16**,** 1113.

Beydoun, M.A., Canas, J.A., Dore, G.A., Beydoun, H.A., Rostant, O.S., Fanelli-Kuczmarski, M.T., Evans, M.K., and Zonderman, A.B. (2016b). Serum Uric Acid and Its Association with Longitudinal Cognitive Change Among Urban Adults. *J Alzheimers Dis* 52**,** 1415-1430.

Beydoun, M.A., Hossain, S., Fanelli-Kuczmarski, M.T., Beydoun, H.A., Canas, J.A., Evans, M.K., and Zonderman, A.B. (2018). Vitamin D Status and Intakes and Their Association With Cognitive Trajectory in a Longitudinal Study of Urban Adults. *J Clin Endocrinol Metab* 103**,** 1654-1668.

Beydoun, M.A., Obhi, H.K., Weiss, J., Canas, J.A., Beydoun, H.A., Evans, M.K., and Zonderman, A.B. (2019). Systemic inflammation is associated with depressive symptoms differentially by sex and race: a longitudinal study of urban adults. *Mol Psychiatry*.

Centers for Disease Control and Prevention (2007). *National Health and Nutrition Examination Surveys 2007-2008: https://wwwn.cdc.gov/nchs/nhanes/continuousnhanes/default.aspx?BeginYear=2007* [Online]. Available: https://wwwn.cdc.gov/nchs/nhanes/continuousnhanes/default.aspx?BeginYear=2007 [Accessed].

Diagnostics, Q. *Ferritin* [Online]. Available: https://www.questdiagnostics.com/testcenter/TestDetail.action?ntc=457&searchString=8272 [Accessed May 13sth 2019].

Diagnostics, Q. *Hemogram* [Online]. Available: https://www.questdiagnostics.com/testcenter/BUOrderInfo.action?tc=7008&labCode=DAL [Accessed May 13sth 2019].

Diagnostics, Q. *Iron, Total and Total Iron Binding Capacity* [Online]. Available: https://www.questdiagnostics.com/testcenter/BUOrderInfo.action?tc=7573&labCode=SEA [Accessed May 13sth 2019].

Doshi, J., Erus, G., Ou, Y., Gaonkar, B., and Davatzikos, C. (2013). Multi-atlas skull-stripping. *Acad Radiol* 20**,** 1566-1576.

Doshi, J., Erus, G., Ou, Y., Resnick, S.M., Gur, R.C., Gur, R.E., Satterthwaite, T.D., Furth, S., Davatzikos, C., and Alzheimer's Neuroimaging, I. (2016). MUSE: MUlti-atlas region Segmentation utilizing Ensembles of registration algorithms and parameters, and locally optimal atlas selection. *Neuroimage* 127**,** 186-195.

Fanelli Kuczmarski, M., Bodt, B.A., Stave Shupe, E., Zonderman, A.B., and Evans, M.K. (2018). Dietary Patterns Associated with Lower 10-Year Atherosclerotic Cardiovascular Disease Risk among Urban African-American and White Adults Consuming Western Diets. *Nutrients* 10.

Fanelli Kuczmarski, M., Mason, M.A., Beydoun, M.A., Allegro, D., Zonderman, A.B., and Evans, M.K. (2013). Dietary patterns and sarcopenia in an urban African American and White population in the United States. *J Nutr Gerontol Geriatr* 32**,** 291-316.

Gunter, J.L., Bernstein, M.A., Borowski, B.J., Ward, C.P., Britson, P.J., Felmlee, J.P., Schuff, N., Weiner, M., and Jack, C.R. (2009). Measurement of MRI scanner performance with the ADNI phantom. *Med Phys* 36**,** 2193-2205.

Hisamatsu, T., Fujiyoshi, A., Miura, K., Ohkubo, T., Kadota, A., Kadowaki, S., Kadowaki, T., Yamamoto, T., Miyagawa, N., Zaid, M., Torii, S., Takashima, N., Murakami, Y., Okamura, T., Horie, M., Ueshima, H., and Group, S.R. (2014). Lipoprotein particle profiles compared with standard lipids in

association with coronary artery calcification in the general Japanese population. *Atherosclerosis* 236**,** 237-243.

Jones, D.K. (2008). Studying connections in the living human brain with diffusion MRI. *Cortex* 44**,** 936-952.

Larsson, A., and Hansson, L.O. (2004). Analysis of inflammatory response in human plasma samples by an automated multicapillary electrophoresis system. *Clin Chem Lab Med* 42**,** 1396-1400.

Li, C., Gore, J.C., and Davatzikos, C. (2014). Multiplicative intrinsic component optimization (MICO) for MRI bias field estimation and tissue segmentation. *Magn Reson Imaging* 32**,** 913-923.

Manickam, P., Rathod, A., Panaich, S., Hari, P., Veeranna, V., Badheka, A., Jacob, S., and Afonso, L. (2011). Comparative prognostic utility of conventional and novel lipid parameters for cardiovascular disease risk prediction: do novel lipid parameters offer an advantage? *J Clin Lipidol* 5**,** 82-90.

Mayo Clinic (2017). *Sed rate (erythrocyte sedimentation rate)* [Online]. Rochester, MN. Available: https://www.mayoclinic.org/tests-procedures/sed-rate/about/pac-20384797 [Accessed May 10th 2019].

Mellen, P.B., Gao Sk Fau - Vitolins, M.Z., Vitolins Mz Fau - Goff, D.C., Jr., and Goff, D.C., Jr. Deteriorating dietary habits among adults with hypertension: DASH dietary accordance, NHANES 1988-1994 and 1999-2004.

Mulkern, R.V., Forbes, P., Dewey, K., Osganian, S., Clark, M., Wong, S., Ramamurthy, U., Kun, L., and Poussaint, T.Y. (2008). Establishment and results of a magnetic resonance quality assurance program for the pediatric brain tumor consortium. *Acad Radiol* 15**,** 1099-1110.

Murakami, K., Livingstone, M.B.E., and Sasaki, S. (2019). Diet quality scores in relation to metabolic risk factors in Japanese adults: a cross-sectional analysis from the 2012 National Health and Nutrition Survey, Japan. *Eur J Nutr* 58**,** 2037-2050.

Murphy, S.P., Foote, J.A., Wilkens, L.R., Basiotis, P.P., Carlson, A., White, K.K., and Yonemori, K.M. (2006). Simple measures of dietary variety are associated with improved dietary quality. *J Am Diet Assoc* 106**,** 425-429.

Myers, J.K., and Weissman, M.M. (1980). Use of a self-report symptom scale to detect depression in a community sample. *Am J Psychiatry* 137**,** 1081-1084.

Nair, D., Carrigan, T.P., Curtin, R.J., Popovic, Z.B., Kuzmiak, S., Schoenhagen, P., Flamm, S.D., and Desai, M.Y. (2009). Association of total cholesterol/ high-density lipoprotein cholesterol ratio with proximal coronary atherosclerosis detected by multislice computed tomography. *Prev Cardiol* 12**,** 19-26.

Nguyen, H.T., Kitner-Triolo, M., Evans, M.K., and Zonderman, A.B. (2004). Factorial invariance of the CES-D in low socioeconomic status African Americans compared with a nationally representative sample. *Psychiatry Res* 126**,** 177-187.

Phantom, N.D.).

Radloff, L. (1977). The CES-D scale: a self-report depression scale for research in the general population. *Applied Psychological Measurement* 1.

Ramos, M.I., Allen, L.H., Haan, M.N., Green, R., and Miller, J.W. (2004). Plasma folate concentrations are associated with depressive symptoms in elderly Latina women despite folic acid fortification. *Am J Clin Nutr* 80**,** 1024-1028.

Samarina, T., and Proskurnin, M. (2015). Rapid assessment of iron in blood plasma and serum by spectrophotometry with cloud-point extraction. *F1000Res* 4**,** 623.

Techs, O.L.C.E.F.C.L.a.M. (2019). Red Blood Cell Distribution Width (RDW): Definition and Calculation.

Tristan-Vega, A., and Aja-Fernandez, S. (2010). DWI filtering using joint information for DTI and HARDI. *Med Image Anal* 14**,** 205-218.

Yin, W., Xu, Z., Sheng, J., Xie, X., and Zhang, C. (2017). Erythrocyte sedimentation rate and fibrinogen concentration of whole blood influences the cellular composition of platelet-rich plasma obtained from centrifugation methods. *Exp Ther Med* 14**,** 1909-1918.

Zou, H. (2006). The adaptive Lasso and it oracle properties. *Journal of the American Statistical Association* 101**,** 1418-1428.